bioRxiv preprint doi: https://doi.org/10.1101/2023.06.20.545721; this version posted November 21, 2023. The copyright holder for this preprint (which was not certified by peer review) is the author/funder, who has granted bioRxiv a license to display the preprint in perpetuity. It is made available under aCC-BY 4.0 International license.

Opportunistic bacteria of grapevine crown galls are equipped with the genomic repertoire for opine utilization

[1,2,#]Hanna Faist, [3,#,]*Markus J. Ankenbrand, [4]Wiebke Sickel, [5,6]Ute Hentschel, [7]Alexander Keller, [2]Rosalia Deeken

[1]AIT Austrian Institute of Technology GmbH, Center for Health & Bioresources, Bioresources Unit, Konrad-Lorenz-Straße 24, 3430 Tulln, Austria

[2]University of Würzburg, Julius-von-Sachs Institute for Biological Sciences, Molecular Plant Physiology and Biophysics, Würzburg, Germany;

[3]University of Würzburg, Faculty of Biology, Center for Computational and Theoretical Biology, Klara-Oppenheimer-Weg 32, Campus Hubland Nord, 97074 Würzburg, Germany;

[4]Thuenen-Institute of Biodiversity, Bundesallee 65, 38116 Braunschweig, Germany;

[5]RD3 Marine Ecology, RU Marine Symbioses, GEOMAR Helmholtz Centre for Ocean Research Kiel, Düsternbrooker Weg 20, 24105 Kiel, Germany;

[6]Christian-Albrechts University of Kiel, Düsternbrooker Weg 20, 24105 Kiel, Germany;

[7]Cellular and Organismic Networks, Faculty of Biology, Ludwig-Maximilians-Universität München, Großhaderner Str. 2-4, 82152 Planegg-Martinsried, Germany;

[#]Both authors contributed equally to this study

*Author for Correspondence: Markus Ankenbrand, Animal Ecology and Tropical Biology, University of Würzburg, Würzburg, Germany, Tel: +49 931 31-85754, Fax: +49 931 31-857540 markus.ankenbrand@uni-wuerzburg.de

bioRxiv preprint doi: https://doi.org/10.1101/2023.06.20.545721; this version posted November 21, 2023. The copyright holder for this preprint (which was not certified by peer review) is the author/funder, who has granted bioRxiv a license to display the preprint in perpetuity. It is made available under aCC-BY 4.0 International license.

Abstract

Young grapevines (*Vitis vinifera*) suffer and eventually can die from the crown gall (CG) disease caused by the plant pathogen *Allorhizobium vitis (Rhizobiaceae)*. Virulent members of *A. vitis* harbour a tumor-inducing (Ti) plasmid and induce formation of crown galls (CGs) due to the oncogenes encoded on the transfer-DNA (T-DNA). Expression of oncogenes in transformed host cells induce unregulated cell proliferation, metabolic and physiological changes. The CG produces opines uncommon to plants, which provide an important nutrient source for *A. vitis* harbouring opine catabolism enzymes. CGs host a distinct bacterial community and the mechanisms establishing a CG-specific bacterial community are currently unknown. Thus, we were interested in whether genes homologous to those of the Ti-plasmid coexist in the genomes of the microbial species coexisting in CGs.

We isolated eight bacterial strains from grapevine CGs, sequenced their genomes and tested their virulence and opine utilization ability in bioassays. In addition, the eight genome sequences were compared to 34 published bacterial genomes, including closely related plant associated bacteria not from CGs. Homologous genes for virulence and opine anabolism were only present in the virulent Rhizobiaceae. By contrast, homologs of the opine catabolism genes were present in all strains including the non-virulent members of the Rhizobiaceae and non-Rhizobiaceae. Gene neighbourhood and sequence identity of the opine degradation cluster of virulent and non-virulent strains together with the results of the opine utilization assay support the important role of opine utilization for co-colonization in CGs, thereby shaping the CG community.

Keywords:

bioRxiv preprint doi: https://doi.org/10.1101/2023.06.20.545721; this version posted November 21, 2023. The copyright holder for this preprint (which was not certified by peer review) is the author/funder, who has granted bioRxiv a license to display the preprint in perpetuity. It is made available under aCC-BY 4.0 International license.

Vitis vinifera, bacterial community, *Agrobacterium*, *Allorhizobium vitis*, Ti-plasmids, *de novo* sequenced genomes

Significance statement:

Virulent *Allorhizobium vitis* causes crown galls on grapevines which reduce plant vigour, yield, and cannot be cured. Non-virulent agrobacteria have been used as biocontrol agents to reduce the virulence potential within a crown gall and disease symptoms. We wanted to know if and how in nature this biocontrol concept is accomplished. We found virulent *Allorhizobium* along with non-virulent *Agrobacterium*, or *Pseudomonas* in the same tumours. Both harboured the catabolism genes in their genomes and metabolized the *quorum sensing* molecule opine. Thus, in nature it seems common that virulent and non-virulent species coexist in a crown gall and that the avirulent members control the virulence potential of the crown gall community by reducing the opine levels.

Introduction

Allorhizobium vitis (*Rhizobiaceae*), former *Agrobacterium vitis* or *Agrobacterium tumefaciens* biovar 3, is the causal pathogen of grapevine crown galls (CGs) which hamper plant growth and yield (Ferreira et al. 1992; Schroth et al. 1988). Overall, the family *Rhizobiaceae* contains both virulent and non-virulent species (Bien et al. 1990; Chandrasekaran et al. 2019) and *Rhizobiaceae* are associated with different grapevine tissues (Burr and Katz 1983). Virulence is encoded by the bacterial tumor-inducing plasmid (Ti-plasmid; Wikipedia contributors 2023) that consists of the transfer DNA (T-DNA), the virulence gene operon (including *vir*-genes), genes encoding opine utilization enzymes as well as a bacterial backbone region that regulates

bioRxiv preprint doi: https://doi.org/10.1101/2023.06.20.545721; this version posted November 21, 2023. The copyright holder for this preprint (which was not certified by peer review) is the author/funder, who has granted bioRxiv a license to display the preprint in perpetuity. It is made available under aCC-BY 4.0 International license.

replication and conjugation of the Ti-Plasmid (Chen and Xie 2011; Gordon and Christie 2014). The Vir-proteins guide the transfer of the T-DNA into the plant nucleus and enable integration into the plant genome. The transformed plant cells express T-DNA encoded genes, consequently leading to the production of plant growth hormones and opines (Gelvin 2010). Uncontrolled production of the plant hormones auxin and cytokinin cause plant cell proliferation and thereby tumorous growth, also referred to as crown galls (CGs; Gohlke and Deeken 2014; Escobar et al. 2001; Klee et al. 1984). CGs do not only offer space for virulent *Rhizobiaceae*, but also for a specific bacterial community which is distinct and differs from the community of a normal wound callus of the graft union (Faist et al. 2016). Moreover, a recent study on the bacterial composition of 73 CGs has shown that at least three non-*A. vitis* groups co-exist in CGs (Gan et al. 2019)

Opines produced by CG cells are a source of nitrogen and carbon for *A. vitis* and the capacity to utilize opines provides a fitness advantage over non-opine utilizing bacteria (Lang et al. 2017). For virulent *Rhizobiaceae*, opines represent not only a nutrient source, but also are involved in *quorum sensing* that regulate e.g., Ti plasmid conjugation and its distribution between bacteria (Ellis et al. 1982; Wetzel et al. 2014). Different virulent *Rhizobiaceae* transfer different opine biosynthesis genes into the plant genome. Various opines are known (Dessaux et al. 1998; Moore et al. 1997; Chilton et al. 2001) and in CGs nopaline, octopine/cucumopine, and/or vitopine/heliopine have been found of which the latter opine-type exclusively occurs in grapevine CGs (Szegedi et al. 1988; Szegedi 2003). It has been postulated that the vitopine/heliopine-type pTi's of *A. vitis* represent a distinct group of Ti-plasmids (Szegedi et al. 1996). Indeed, the bacterial catabolism genes on the Ti-plasmid correspond to these opine-types. Nevertheless, as opines are produced by T-DNA transformed plant cells, they are a public good in a CG (Platt et al. 2012). Consequently, other bacteria of the CG community may also utilize opines as a nutrient source, promoting their enrichment in CGs. For example, some

bioRxiv preprint doi: https://doi.org/10.1101/2023.06.20.545721; this version posted November 21, 2023. The copyright holder for this preprint (which was not certified by peer review) is the author/funder, who has granted bioRxiv a license to display the preprint in perpetuity. It is made available under aCC-BY 4.0 International license.

Pseudomonas strains isolated from CGs can utilize opines (Bergeron et al. 1990; Moore et al. 1997).

In our study, we provide the draft genome sequences of three virulent *A. vitis* isolates and five non-virulent bacterial isolates of grapevine CG communities (three *Rhizobiaceae*, one *Pseudomonas* and one *Rahnella*) and analysed these strains for virulence. In octopine and nopaline utilization bioassays we tested growth of the eight grapevine CG isolates. In addition, 34 published genomes of plant associated bacteria were included in our analyses to identify orthologous genes of the Ti-Plasmids. In our genome analysis, we focussed on the distribution of genes involved in virulence, Ti-plasmid conjugation (quorum sensing), and opine metabolism in the CG bacterial communities.

Results

Physical characteristics of the eight genomes

The eight *de novo* sequenced bacterial genomes belonged to isolates from five different grapevine CGs harvested in the region Franconia, Bavaria, Germany (supplementary table S1). According to EZBioCloud (Yoon, et al. 2017) the isolates CG1-CG6 belonged to the *Rhizobiaceae* family, CG7 was identified as *Pseudomonas sp.*, and CG8 as *Rahnella sp.* (supplementary table S1). The screening for amplicon sequencing variants (ASVs) of the dataset published by Faist et al. 2016 revealed that the V4 regions of the 16S rRNA sequences from the isolates CG1-CG3 and CG7-CG8 were significantly enriched in CGs compared to healthy graft unions (table 1) whereasASVs of CG4-CG6 showed no significant enrichment (Faist et al. 2016).

bioRxiv preprint doi: https://doi.org/10.1101/2023.06.20.545721; this version posted November 21, 2023. The copyright holder for this preprint (which was not certified by peer review) is the author/funder, who has granted bioRxiv a license to display the preprint in perpetuity. It is made available under aCC-BY 4.0 International license.

The general features of the assembled eight draft genomes are summarized in supplementary table S2. The length of the smallest contigs, which accounted for 90% of the genome (N90 index), ranged from 17.6 kb (CG7, *Pseudomonas*) to 204 kb (CG6, *Rhizobiaceae sp.*). The *A. vitis* draft genomes (CG1-CG3) shared a GC content of around 57%, while it varied between the other *Rhizobiaceae* isolates (CG4-CG7, 55-61.5%). *Rahnella* (CG8) possessed the lowest GC content with 52.3%. Mapping the raw reads to the draft genomes resulted in ~98% alignment rates for CG1, CG2, CG4-CG6 and about ~85-87% for the isolates CG3, CG7, and CG8.

Inoculation assays demonstrated that the three *A. vitis* isolates (CG1-CG3) induced CG development on stems of in vitro cultivated grapevine plantlets but not the other three Rhizobiaceae isolates (CG4-CG6; supplementary fig. 1). Like the latter three, *Pseudomonas* (CG7) and *Rahnella* (CG8) did not induce CG development even in stems of the test plants *Arabidopsis thaliana* and *Nicotiana benthamiana*. Thus, the isolates CG1-CG3 were confirmed as virulent, while CG4-CG8 were non-virulent.

Relationship between isolates and reference genomes

Information about the selection criteria of the *de novo* sequenced draft genomes (CG1-CG8) and the reference sequences of known plant associated bacteria used for phylogenetic relationship analysis are summarized in table 1. The numbers of predicted coding sequences (CDS) and tRNAs are similar among the isolates while the number of rRNAs varies, most likely due to the highly challenging assembly of frequently duplicated genes in draft genomes. At least 103 out of 107 essential genes were found in all *de novo* sequenced isolates indicating a completeness of the draft genomes of at least 96%.

The *Rhizobiaceae* family encompasses virulent and non-virulent members including the monophyletic groups of *Agrobacterium* and *Allorhizobium* (Gan and Savka 2018). The results

bioRxiv preprint doi: https://doi.org/10.1101/2023.06.20.545721; this version posted November 21, 2023. The copyright holder for this preprint (which was not certified by peer review) is the author/funder, who has granted bioRxiv a license to display the preprint in perpetuity. It is made available under aCC-BY 4.0 International license.

of a phylogenetic tree generated on the basis of 107 housekeeping gene sequences revealed that the two non-virulent *Rhizobiaceae* isolates CG4 *(A. divergens)* as well as CG6 (*A. rosae*) belong to the clade of *Agrobacterium* while CG5 is related to *Allorhizobium* (supplementary fig. 2). The three virulentisolates CG1-CG3 formed a clade also with the genus *Allorhizobium* of which CG2-CG3 belonged to the branch of *A. vitis*. A whole genome alignment using the program AliTV performed with *A. ampelinum* and the draft genomes of the isolates CG1-GC3 revealed that the two chromosomes and the pATS4e plasmid express high homology (fig. 1, green connecting lines, >85% homology), while the pTiS4 plasmid possessed much lower homology (orange to yellow connecting lines, <85% homology). The close relationship between the virulent *A. vitis* genomes was confirmed by the number of protein families shared (fig. 2). CG1, CG2, and CG3 exclusively shared 211 protein families with *A. ampelinum* and *A. vitis* NCPPB3554 (K309) (fig. 2, arrow).

Relationships between isolates and reference Ti plasmids

The relationship between Ti-plasmids was investigated by aligning the potential pTi sequences of our *de novo* sequenced strains with each other and with the reference sequences of pTiS4 (vitopine/heliopine-type), pTiAg57 (octopine/cucumopine-type), pTiC58 (nopaline-type), and pTiK309 (octopine-type). The potential Ti-plasmids of the sequenced isolates CG1, CG2, and CG3 are more homologous to each other than to the reference pTi sequences. Among the three, CG2 and CG3 show a higher degree of homology to each other than to CG1 (fig. 3*A*). The alignments of CG1-CG3 to the reference pTis revealed that large parts of the CG1 contigs have strong homology (more than 99% identity) to long regions of pTiAg57 and almost the complete pTiK309 sequence (fig. 3*B*, dark green connecting lines). In particular, the *vir*-regions (fig. 3*B-D*, green bars) of the *de novo* sequenced *Allorhizobium* isolates (CG1-CG3) are highly homologous (100%) to the *vir*-regions of pTiAg57 and pTiK309 but much less to pTiS4 (orange connecting lines) and pTiC58 (red connecting lines). Furthermore, other contigs of CG1-CG3

bioRxiv preprint doi: https://doi.org/10.1101/2023.06.20.545721; this version posted November 21, 2023. The copyright holder for this preprint (which was not certified by peer review) is the author/funder, who has granted bioRxiv a license to display the preprint in perpetuity. It is made available under aCC-BY 4.0 International license.

encoding opine synthesis (fig. 3 purple bars), opine utilization and transport (fig. 3, grey bars), as well as plasmid replication and transfer (fig. 3, yellow bars) match to a high degree to pTiAg57.

Prediction of Ti-Plasmid encoding protein families

To functionally describe the *de novo* sequenced genomes of the eight CG isolates, we compared the predicted protein sequences with those of the reference strains. The predicted proteins were clustered into orthologous groups (in short: orthogroups) by a set of amino acid sequences derived from a single common ancestor sequence for all the isolates (Emms and Kelly 2015). In total 21,431 unique predicted orthogroups were identified and for a selection of 15 plant associated bacteria, including the eight CG isolates and seven of the reference genomes, 495 orthogroups were shared by all the isolates (fig. 4). The genomes of the *Rhizobiaceae* had 349 additional unique orthogroups in common, and the taxonomically heterogeneous genomes of crown gall-associated bacteria shared only a single unique orthogroup. However, the subgroup of virulent bacterial genomes exclusively shared 28 orthogroups with each other.

The proteins known to be encoded by the Ti-plasmids (pTiC58, pTiS4, pTiK309, pTiAg57) of the reference bacteria *A. tumefaciens* C58, *A. ampelinum, A. vitis* NCPPB3554, and *A. fabrum* Ag57, respectively are listed in table 2 and assigned to all of our isolates CG1-CG8. The predicted protein families functioning in virulence and CG induction were present in the genomes of the three virulent isolates CG1-CG3 but largely absent in the genomes of the non-virulent bacteria (table 2A). An exception was VirG which is part of the sensory response system and therefore found in all analysed genomes in substantial numbers. Proteins related to plasmid replication and transfer (Tra, Trb, RepABC) were not only present in the virulent CG1-CG3 but also in the non-virulent isolates CG4, CG5 and CG6, while they were missing in *Pseudomonas sp.* (CG7) and *Rhanella sp.* (CG8) (table 2B). Protein families predicted to be

bioRxiv preprint doi: https://doi.org/10.1101/2023.06.20.545721; this version posted November 21, 2023. The copyright holder for this preprint (which was not certified by peer review) is the author/funder, who has granted bioRxiv a license to display the preprint in perpetuity. It is made available under aCC-BY 4.0 International license.

associated with opine utilization such as opine catabolism (OoxA/B, NoxA/B, VoxA/B) occurred in all analysed genomes (table 2C) and were not unique to the virulent bacteria in contrast to those for opine anabolism (Vis, Cus, Ocs, Acs, Acsx). Proteins functioning in opine transport (e.g. AccC-E and OccPch, NocP) were found in large numbers. Taken together, virulence, opine degradation, and T-DNA encoded protein families were predominantly found in the genomes of the virulent *A. vitis* isolates. Those predicted to transfer and replicate Ti-plasmids were present in all *Rhizobiaceae* isolates and proteins for opine transport and catabolism occurred in all listed plant associated bacteria.

Genetic basis for opine utilization match *in vitro* opine bioassay

All CG associated isolates, except CG4, contained representatives of the well-described Nox/Oox/Vox protein families, essential for opine degradation. Figure 5 visualizes the order and orientation of the predicted proteins in the vicinity of the subunits A and B ofOox/Nox/Vox (green and turquoise arrows) in the *de novo* sequenced genomes and the reference *A. vitis* NCPPB3554 (K309). The fragments of the virulent *A. vitis* isolates CG1-CG3 showed exactly the same structure as the reference. This included the NoxA/B, OoxA/B, and VoxA/B protein families (fig. 5, green and turquoise arrows), other protein families related to opine catabolism (fig. 5, pale green arrows) and those for opine transport (fig. 5, blue arrows) upstream of OoxB/NoxB/VoxB (fig. 5, green arrows). Isolate CG1 harboured a second cluster with additional genes between the transport protein family and OoxB/NoxB/VoxB. Growth assays with the virulent CG1-CG3 isolates in liquid AB salt medium supplemented with opines as sole carbon and nitrogen source, confirmed the function of the opine catabolism clusters (supplementary table S3) The isolates utilized octopine better than nopaline pointing to the presence of octopine catabolism gene clusters in their genomes.

bioRxiv preprint doi: https://doi.org/10.1101/2023.06.20.545721; this version posted November 21, 2023. The copyright holder for this preprint (which was not certified by peer review) is the author/funder, who has granted bioRxiv a license to display the preprint in perpetuity. It is made available under aCC-BY 4.0 International license.

The three non-virulent *Rhizobiaceae* isolates CG4, CG5, and CG6 showed a different behaviour concerning opine utilization. *A. divergens* (CG4) did not grow, but *Rhizobiaceae sp. (*CG5) grew well and *A. rosae* (CG6) weakly in liquid AB salt medium supplemented with octopine (supplementary table S3). Accordingly, the opine degradation region of CG4 lacked all substantial components (Fig. 5, black line) while the two clusters of CG5 harboured the essential genes, however, in a different order as compared to the virulent isolates CG1-CG3, except of the Nox/Oox/Vox proteins (fig. 5). CG6 possessed the same opine cluster structure as the *A. vitis* NCPPB3554 (K309) reference strain and the virulent isolates *A. vitis* CG1-CG3 but grew only weekly in opine containing liquid medium (supplementary table S3). A closer inspection of CG6 revealed additional predicted protein sequences that were homologous to those of the isolate CG1 and the reference plasmid pTiC58 of *A. fabrum* C58 (fig. 6A). In the reference plasmid, the homologs were related to replication and regulation of transfer (yellow bars), Ti plasmid transfer (orange bars), and opine utilization and transport (grey bars). Regions related to virulence (green bars) and the T-DNA (red bars) were not detected in the isolate CG6 genome but in the isolate CG1. This underlined the finding that CG6 was unable to induce CGs (supplementary fig. 1) but able to metabolize octopine, although not very well (supplementary table S3). Therefore, we compared the opine utilization and transport regions of CG6 also with the non-virulent agrocinopine/nopaline-type plasmid pAtK84b of *A. rhizogenes K84* and the octopine/cucumopine-catabolic *A. fabrum* plasmid pAtAg67 of the narrow host range *A. fabrum* strain Ag57. We found higher sequence identity between those than between CG6 and the Ti plasmid of C58 (fig. 6B, green connecting lines between grey bars). Particularly, one contig of CG6 matched the cucumopine-catabolic region of pAtAg67 with 99.5% identity. Thus, it is likely that the opine utilization and transport region of CG6 belongs to an opine-catabolic plasmid, most likely a cucumopine-type, rather than to a Ti plasmid.

bioRxiv preprint doi: https://doi.org/10.1101/2023.06.20.545721; this version posted November 21, 2023. The copyright holder for this preprint (which was not certified by peer review) is the author/funder, who has granted bioRxiv a license to display the preprint in perpetuity. It is made available under aCC-BY 4.0 International license.

The draft genome of the *Pseudomonas* isolate CG7 contained three regions with homology to the OoxA/B, NoxA/B, VoxA/B protein families, none of them has all the genes like the reference (NCPPB3554; fig. 5). However, the CG7 isolate grew well in liquid AB salt medium containing octopine like *A. rosa* CG6 and despite the differences in the structure of the opine clusters to those of the virulent isolates CG1-CG3 (supplementary table S3). In the *Rahnella* CG8 genome the DNA sequences encoding the OoxB/NoxB/VoxB protein family were also present in the classical orientation upstream of OoxA/NoxA/VoxA (fig. 5). However, in contrast to the opine-utilization clusters of CG1-CG3, the opine-transporter genes (fig. 5, blue arrows) in CG8 were downstream of OoxA/B, NoxA/B, VoxA/B and the isolate was not able to metabolize opines (supplementary table S3). Taken together, our study reveals that the non-virulent CG-associated bacteria *A. rosae* CG6 and *Pseudomonas* CG7 possess functional opine transport and catabolism sequence regions.

Discussion

Virulent *Allorhizobium vitis* strains generate a new ecological niche in plants by transferring a T-DNA into the plant genome that leads to neoplastic growth of grapevine tissue so-called crown galls (CGs). In contrast to normal stem tissues, CGs form a sink tissue characterized by a hypoxic environment and accumulation of sugars, amino acids, and opines (Deeken, et al. 2006) which are exclusively produced by T-DNA harbouring host cells. In addition to the pathogen, a seasonally stable microbiota resides in the nutrient-rich CG environment (Faist et al. 2016).

This study aims to unravel whether homologs of the protein-encoding genes typically located on the Ti-plasmid of virulent agrobacteria are also found in non-virulent bacterial members of the CG bacterial community. To identify these genes in CG associated bacteria, we included

bioRxiv preprint doi: https://doi.org/10.1101/2023.06.20.545721; this version posted November 21, 2023. The copyright holder for this preprint (which was not certified by peer review) is the author/funder, who has granted bioRxiv a license to display the preprint in perpetuity. It is made available under aCC-BY 4.0 International license.

genomes of non-tumour-associated plant bacteria in our analysis. Thereby we focussed on the functions: virulence, plasmid replication and transfer (conjugation), as well as opine utilization summarized in table 2. The distribution of the underlying genes may allow us to draw conclusions regarding the importance of their role in CG ecology.

Virulence is restricted to *A. vitis* in the CG community

Three out of the eight *de novo* sequenced bacterial isolates (CG1, CG2, CG3) analysed in this study belonged to the taxonomic group of *Allorhizobium* . They were isolated from different grapevine CGs and in an infection assay they induced neoplastic growth on *in vitro* cultivated grapevines. The sequences comprising the chromosomes of CG1-CG3 were largely homologous to those of the well characterized strain *A. ampelinum* (fig. 1). Concerning the Ti-plasmid sequences the three genomes showed a higher homology to each other than to the reference Ti-plasmids of *A. ampelinum* (vitopine/heliopine-type), *A. fabrum* Ag57 (octopine/cucumopine-type), *A. fabrum* C58 (nopaline-type), and *A. vitis* pTiK309 (octopine-type fig. 3). The Ti-plasmid pTiAg57 was more similar to the putative plasmid contigs of CG2 and CG3, than any of the other reference plasmids (pTiS4, pTiC58, pTiK309). These findings support the idea of i) an independent propagation of th chromosomes and Ti-plasmids, as previously suggested (Slater et al. 2009) and ii) a faster ecological specification of plasmids encoding virulence in contrast to chromosomes encoding mainly housekeeping functions (Weisberg et al. 2020). Both factors must be considered for the development and interpretation of diagnostic tests targeting the CG disease.

Essential for CG development are the virulence regions located on the Ti-plasmid, that are involved in the process of T-DNA transformation and have previously been summarized for *A. fabrum C58* (Pitzschke and Hirt 2010). Our *A. vitis* isolates CG1-CG3 shared similar predicted protein sequences associated with virulence of the Ti plasmids of *A. fabrum* C58 (pTiC58), *A.*

bioRxiv preprint doi: https://doi.org/10.1101/2023.06.20.545721; this version posted November 21, 2023. The copyright holder for this preprint (which was not certified by peer review) is the author/funder, who has granted bioRxiv a license to display the preprint in perpetuity. It is made available under aCC-BY 4.0 International license.

284 *ampelinum* (pTiS4), *A. vitis* NCPPB3554 (pTiK309) and *A. fabrum* Ag57 (pTiAg57). Among
285 those are the proteins known to be important for (i) recognition of the host cell and induction
286 of Vir gene expression (VirA, VirG), (ii) the type IV secretion system (T4SS: VirB2, VirB5,
287 VirB6, VirD4, etc.) for the transfer of the T-DNA (Tra and trb genes), and (iii) T-DNA
288 integration (VirC2, VirE2, VirE3, VirD5, etc.) into the plant genome (table 2A).

289 The VirA and VirG protein families involved in host recognition were detected in all but CG8
290 (no VirA) *de novo* sequenced virulent and non-virulent genomes as well as the three reference
291 genomes. For *A. fabrum* C58 it is known that the ubiquitously expressed two-way component
292 phospho-relay system VirA/VirG detects and transduces signals of wounded plants and the
293 phosphorylated VirG activates transcription of the Vir operon (Brencic and Winans 2005; Wise
294 and Binns 2015). Nevertheless, VirG belongs to a large family of positive regulators responding
295 to external phenolics, monosaccharides and pH (Winans et al. 1986), indicating that the
296 predicted protein family plays multiple roles besides virulence regulation.

297 The agrobacterial VirB/VirD4 system forms the T4SS, dedicated to deliver the T-DNA and
298 effector proteins into plant cells in the course of infection. Most protein homologs of the T4SS
299 encoded on the three reference Ti plasmids (pTiC58, pTiS4, pTiK309,pTiAg57) were present
300 in the virulent *A. vitis* isolates (CG1-CG3). However, our virulent isolates harbour most likely
301 a T4SS variant distinct from the one of the reference Ti plasmids because sequences encoding
302 VirB7, VirB8, VirB9 were not present in the genome data of CG1-CG3. These Vir proteins
303 have stabilizing functions and are either located in or at the outer (VirB7, VirB9) as well as
304 inner (VirB8) bacterial membrane (Gordon and Christie 2014).

305 The agrobacterial factors translocated into host cells by the T4SS are essential for T-DNA
306 integration and include the VirD2-T-DNA complex, VirD5, VirE2, VirE3, and VirF (Vergunst
307 et al 2005; Schrammeijer et al. 2003). These protein families have different functions and were

bioRxiv preprint doi: https://doi.org/10.1101/2023.06.20.545721; this version posted November 21, 2023. The copyright holder for this preprint (which was not certified by peer review) is the author/funder, who has granted bioRxiv a license to display the preprint in perpetuity. It is made available under aCC-BY 4.0 International license.

present in the genomes of our virulent isolates CG1-CG3. Taken together, the genome sequences of our *A. vitis* isolates CG1-CG3 harbour the genetic repertoire required to cause CG disease (supplementary fig. 1).

All *Rhizobiaceae* isolates harbour the machinery for Ti-plasmid conjugation

CGs are a perfect niche for plasmid conjugation within a bacterial population (Dessaux and Faure 2018). The proteins necessary for replication (RepABC) and transfer (Tra, Trb) of Ti-plasmids have been previously described in detail (Lang and Faure 2014). Representatives of these protein families existed in our virulent and non-virulent *Rhizobiaceae* genomes (table 2B), but not in the - isolates CG7 (*Pseudomonas sp.*) and CG8 (*Rahnella sp.*) that were also part of the CG microbiota (Faist et al. 2016). The genomes of the three virulent *A. vitis* isolates (CG1-CG3) each contained a region (fig. 3*B-D*, black arrow heads) coding for pTi replication (yellow bars) and transfer (orange bars) which had highest homology to pTiAg57 of *A. fabrum* Ag57 (≤ 100%, green connecting lines), less homology to pTiC58 of *A. fabrum* C58, pTi309 of *A. vitis* NCPPB3554 (≤ 90%, pale green connecting lines), and least to pTiS4 of *A. ampelinum* (≤ 80%, orange connecting lines). Among the non-virulent *Rhizobiaceae* isolates, CG4 (*A. divergens*) and CG5 (*Rhizobium sp.*) seem to lack the sequence encoding replicase RepC based on the orthologue prediction (table 2) . However, the automatic gene annotation by NCBI revealed multiple genes classified as repC. This indicates the limitation of our gene assignment method, which can lead to false negatives. The also non-virulent *Rhizobiaceae* isolate CG6 (*A. rosae*) contained an almost identical sequence region to the virulent isolate *A. vitis* CG1 (fig. 6A, green connecting line) involved in plasmid replication (yellow bars) and transfer (orange bars) suggesting the presence of a plasmid, but not of a virulent Ti-plasmid. Regions involved in virulence (green bars) and T-DNA transfer (red bars), found in the genomes of C58 and CG1 were lacking in CG6.

bioRxiv preprint doi: https://doi.org/10.1101/2023.06.20.545721; this version posted November 21, 2023. The copyright holder for this preprint (which was not certified by peer review) is the author/funder, who has granted bioRxiv a license to display the preprint in perpetuity. It is made available under aCC-BY 4.0 International license.

Quorum sensing and *quorum quenching* regulate conjugation of Ti-plasmids between bacteria and horizontal transfer of the T-DNA into the host genome (Dessaux and Faure 2018). Opines synthesized by T-DNA transformed tumour cells play a key role in bacterial conjugation since they activate the conjugal transfer (*tra*) genes (Mel and Mekalanos 1996). Sequences of the predicted protein families involved in *quorum sensing* (TraI, TraM TraR) were present in all virulent and non-virulent *Rhizobiaceae* genomes (table 2B), but not in *Pseudomonas* sp. (CG7) and *Rahnella sp.* (CG8). The fact that similar *quorum sensing* genes existed in the virulent and non-virulent *Rhizobiaceae* isolates raised the possibility of cross species communication. This seems likely between our virulent *A. vitis* (CG2) and non-virulent *Pseudomonas* (CG7) isolates as well as between *A. vitis* (CG3) and *Rahnella* (CG8) because these resided in the same tumour B and tumour C, respectively (supplementary table S3). Representatives of the lactonase protein families (AttM/BlcC, AiiB) which degrade the bacterial *quorum sensing* signal molecule N-acyl homoserine lactone and thus are functioning in *quorum quenching* were found in the virulent *A. vitis* (CG1), the non-virulent *A. rosae* (CG6), and *Pseudomonas* (CG7; table 2C). *Quorum quenching* reduces the Ti-plasmid transfer frequency and thereby the host transformation events by virulent agrobacteria (Haudecoeur et al. 2009; Haudecoeur and Faure, 2010; Lang et al. 2016). Since *A. vitis* CG1, *A. rosae* CG6 and *Pseudomonas* CG7 were from different CGs they cannot negatively influence plasmid conjugation among each other or between *Rahnella* (CG8) and *A. vitis* (CG3) and *Pseudomonas* (CG7) and *A. vitis* (CG2). Thus, the latter two isolate pairs of tumour B and C, each have the genetic repertoire to communicate via *quorum sensing* signals and transfer genetic material.

Opine utilization plays a key role in CG colonization

The possibility for non-virulent bacteria to acquire the ability for opine utilization is advantageous for them in the CG environment. An overview of the genes involved in opine utilization by agrobacteria is provided in Vladimirov et al. 2015 and table 2C. In CGs, different

bioRxiv preprint doi: https://doi.org/10.1101/2023.06.20.545721; this version posted November 21, 2023. The copyright holder for this preprint (which was not certified by peer review) is the author/funder, who has granted bioRxiv a license to display the preprint in perpetuity. It is made available under aCC-BY 4.0 International license.

357 opines can coexist (Petit et al. 1983) and their recognition is conferred by various periplasmic
358 binding proteins (PBPs). The PBPs OccT and NocT can recognize nopaline and octopine,
359 respectively or in the case of NocT even both opines (Vigouroux et al. 2017). Association of
360 PBPs with ATP binding cassette transporters (OocQ, NocQ, OocM, NocM, OccP, NocP)
361 enables the import of opines into bacterial cells (Zanker et al. 1992). In our study NocT, OccT
362 homologs were present in all crown gall-associated genomes and representatives of the ABC
363 transporters (OccPch, NocP1 and OccQe, OccMch, etc.) even in high copy numbers (table 2C).
364 A similar ubiquitous occurrence showed protein families for opine sensing (NocR, AccR).
365 These function in transcriptional activation of opine uptake and catabolism genes (Subramoni
366 et al. 2014). Hence, all crown gall-associated bacteria harbour the genetic potential for opine
367 uptake and sensing.

368 Ti plasmids carry the genes for opine synthesis (*nos*, *ocs*, *vis*, cus, acs, etc.) by plant cells as
369 well as the corresponding catabolism genes (*noxA*/*noxB*, *ooxA*/*ooxB*, rocF etc.). The octopine
370 synthase gene sequence (*ocs*) is similar to the one of vitopine synthase (*vis*) and therefore joins
371 the same protein family while the nopaline synthase gene (*nos*) forms a separate family
372 (Canaday et al. 1992). We found homologs of the opine synthases Ocs, Vis, Cus, and Acs/AcsX
373 but not Nos, Nos-like, and Mas1 in the genomes of the virulent isolates GC1-GC3 only (table
374 2C). Since no Nos/Nos-like homologs were found in the genomes of isolates CG1-CG3 and
375 these metabolized octopine much better than nopaline (supplementary table S3) we suggest that
376 our three virulent *A. vitis* isolates harbour an octopine/vitopine-type Ti plasmid rather than a
377 nopaline-type.

378 In contrast to anabolism, which was restricted to the virulent isolates, all analysed crown gall-
379 associated bacterial genomes harboured sequences encoding enzymes for opine catabolism
380 (table 2C). The protein families of OoxA/NoxA and OoxB/NoxB were found in all genomes,
381 except of the isolate CG4 (*A. divergens*) which lacked OoxB/NoxB. OoxA/NoxA together with

bioRxiv preprint doi: https://doi.org/10.1101/2023.06.20.545721; this version posted November 21, 2023. The copyright holder for this preprint (which was not certified by peer review) is the author/funder, who has granted bioRxiv a license to display the preprint in perpetuity. It is made available under aCC-BY 4.0 International license.

382 OoxB/NoxB are two soluble polypeptides, which are both required for the first step of opine
383 utilization (Zanker, et al. 1994) and may explain why CG4 could not metabolise nopaline or
384 octopine (supplementary table S3). Furthermore, the arrangement of the genes encoding the
385 proteins for opine catabolism is essential for an effective function (Zanker, et al. 1994). The
386 order and orientation of the genes involved in opine sensing (*nocR*), uptake (*occQe, occPch,*
387 *nocP*) and catabolism (*ooxB, rocF, ocd*) in the vicinity of *ooxB/ooxA* of the type IVb reference
388 Ti-plasmid of *A. vitis* NCPPB3554 (fig. 5) was the same in our virulent isolates (CG1-CG3). It
389 differed in the genomes of the non-virulent isolates CG4, CG5, CG7, and CG8, but not CG6.
390 *Rhizobiaceae sp.* CG5 metabolized octopine well and harboured the essential catabolism genes
391 *ooxA* and *ooxB* in the correct order and orientation but the other genes in some distance. The
392 gene order and orientation in the genome of *A. rosae* CG6 was the same as in the virulent
393 isolates. This points to a different event of acquisition for the opine transport and catabolism
394 genes and might have an impact on opine utilization which was less effective by CG6 compared
395 to the virulent isolates CG1-CG3. The sequences for opine transport and catabolism of CG6
396 revealed a high degree of similarity to the pAtK84b plasmid of the strain *A. rhizogenes* K84
397 and an even higher to the pAtAg67 plasmid from *A. fabrum* Ag57 (fig. 6B, grey bars). *A.*
398 *rhizogenes* K84 harbours a nopaline-catabolic plasmid (pAtK84b) and *A. fabrum* Ag57 an
399 octopine/cucumopine-catabolic plasmid (pAtAg67; Hooykaas et al., 2022) which lack the Vir
400 and T-DNA regions like the genome of CG6. *A. rhizogenes* K84 is frequently used as biocontrol
401 agents to prevent CG development (Clare et al. 1990). Thus, OC plasmids have an ecological
402 impact on controlling CG disease severity, possibly via advantages in the competition for opines
403 with virulent strains and the secretion of antimicrobial substances (Platt et al. 2014).

404 The *Pseudomonas* isolate CG7 contained two regions which showed the essential succession
405 of *ooxA/noxA* and *ooxB/noxB* but lacked sequences for *arc*, *odh*, and *ocd/rolD* (fig. 5).
406 Nevertheless, the *in vitro* growth assay confirmed utilization of octopine by *Pseudomonas* CG7.

bioRxiv preprint doi: https://doi.org/10.1101/2023.06.20.545721; this version posted November 21, 2023. The copyright holder for this preprint (which was not certified by peer review) is the author/funder, who has granted bioRxiv a license to display the preprint in perpetuity. It is made available under aCC-BY 4.0 International license.

Previously it was shown that in CGs of grapevines bacteria other than *A. vitis* can utilize opines, including *Pseudomonas* strains (Canfield and Moore 1991; Nautiyal and Dion 1990; Moore et al. 1997; Wetzel et al. 2014; Eng et al. 2015). However, the molecular mechanism behind it is yet unknown. The *Rahnella* isolate CG8 harboured the essential genes for opine catabolism but those for opine transport were located downstream of *ooxA/noxA* and *ooxB/noxB* (fig. 5). Therefore, one might speculate that the reversed order of the essential opine-catabolic and uptake genes may prevent opine utilization by Rahnella (CG8). The reference genome of *Rahnella aquatillis* HX2 (No. 34 in table 1) does also not harbour the essential genes for opine utilization and was proposed to function as biocontrol in confining CG disease (Chen et al. 2007). Consequently, the non-virulent CG isolates *Rhizobiaceae sp.* CG6, *Pseudomonas* CG7, and *Rahnella* CG8 have the potential to control CG disease.

In root nodules, acquisition events have previously been suggested between Alpha-, Beta- and Gammaproteobacteria (Shiraishi et al. 2010; Ryu et al. 2020; De Meyer et al. 2016). Thus, an exchange of gene sequences between our alphaproteobacterium *A. vitis* (CG1, CG2, CG3), betaproteobacterium *Rahnella* (CG8), and the gammaproteobacterium, *Pseudomonas* (CG7) seems possible in CGs since CG2 and CG7 as well as CG3 and CG8 resided in the same CG. This might equip the non-virulent members of the microbial CG community with the machinery to utilize opines. Moreover, the transfer of the opine utilization machinery to beneficial plant bacteria could stabilize their population in an opine enriched environment. Taken together, in CGs, virulent *Rhizobiaceae* provide an opine-rich niche for themselves and other opine catabolizing bacteria as well.

Conclusion

On a genetic level, gene duplication, rearrangements and interspecies horizontal gene transfer may be important for the dissemination of opine utilization among the CG-associated bacterial

bioRxiv preprint doi: https://doi.org/10.1101/2023.06.20.545721; this version posted November 21, 2023. The copyright holder for this preprint (which was not certified by peer review) is the author/funder, who has granted bioRxiv a license to display the preprint in perpetuity. It is made available under aCC-BY 4.0 International license.

community. Our results highlight the distribution of sequences encoding proteins for opine catabolism (utilization of the CG-specific nutrient), but not for virulence (induction of the CG disease) among the bacterial community of the CG. The extent of CG development correlates with the number of transformation events and plant vigour. Grapevines developing small CGs show no growth limitations (Ferreira et al. 1992; Schroth et al. 1988) and the grapevines of this study did also not display an obvious phenotype. Opines are unique compounds produced by CGs which can only be metabolized by bacteria expressing enzymes for opine uptake and degradation. In contrast, other plant nutrients must be shared by the whole CG community. Competition for opines between virulent *A. vitis* and non-virulent bacteria could balance the composition of the microbial community in a CG and thus, promote or limit the degree of the CG disease. Therefore, a better understanding of the factors balancing the composition of the microbial community and providing a bacterial community, which is dominated by beneficial microbes, might lead to novel disease management strategies.

Material and Methods

Isolation and cultivation of bacteria

In 2011, 2012 and 2013 we isolated bacteria from CG material sampled in vineyards of Franconia, Germany. The grapevine cultivars consisted of the scion Cabernet Dorsa, Scheurebe and Müller Thurgau grafted onto the rootstocks 5BB and SO4 (NCBI, BioProject: PRJNA624984). CG material was ground (2 min, 30 Hz) using a ball mill (Retsch, Hannover, Germany) and 300 mg CG powder was suspended in super purified water (RotisolV high-performance liquid chromatography [HPLC] gradient grade; Roth). After incubation for 2 h at 28°C, the supernatant was used for 10-fold serial dilutions. Agar plates containing yeast extract broth (YEB; 0.5% [wt/vol] tryptone, 0.5% [wt/vol] yeast extract, 0.5% [wt/vol] sucrose, 1.23%

bioRxiv preprint doi: https://doi.org/10.1101/2023.06.20.545721; this version posted November 21, 2023. The copyright holder for this preprint (which was not certified by peer review) is the author/funder, who has granted bioRxiv a license to display the preprint in perpetuity. It is made available under aCC-BY 4.0 International license.

455 [wt/vol] MgSO4 [AppliChem, Darmstadt, Germany], 1.5% [wt/vol] Agar-Agar Kobe I [Carl-
456 Roth, Karlsruhe, Germany]) supplemented with 213 µM cycloheximide (CHX; Sigma-Aldrich,
457 St. Louis, MO, USA) were used for bacterial growth at 28°C. By growing colonies on
458 rifampicin containing yeast extract agar (RIF-YEA, 10 µg/ml) plates, spontaneous rifampicin-
459 resistant derivatives were selected for tracking them in their natural environment. Single
460 colonies were sub-cultured at least five-times on YEA-CHX-RIF plates and used for *de novo*
461 shotgun sequencing.

462 **Virulence and opine growth assays**

463 Virulence assays were performed by inoculating bacterial suspensions into *Vitis vinifera* stems
464 as described by Faist et al. 2016, stems of four weeks old *Arabidopsis thaliana* (accession Col-
465 0), and *Nicotiana benthamiana* plants according to (Gohlke et al. 2013). Pictures were taken
466 using a CCD camera (Leica DFC500, Leica Microsystems GmbH) attached to a stereo
467 microscope (Leica MZFLIII, Leica Microsystems GmbH). Opine utilization assays were
468 performed in liquid AB minimal medium (K2HPO4 3 g/L; NaH2PO4 1 g/L; MgSO4-7H2O 0.3
469 g/L; KCl 0.15 g/L; CaCl2 0.01 g/L; FeS04-7H2O 2.5 mg/L; pH 7) supplemented with 1 mg/ml
470 octopine or nopaline (Vigouroux et al. 2017) or with sucrose+NH_4 and glycerol as controls.
471 Bacterial growth was determined as optical density (OD_{600}) and defined as follows: no growth,
472 $OD < 0.1$; very weak growth, $0.1 \leq OD < 0.2$; weak growth $0.2 \leq OD < 0.5$; growth $OD \geq 0.5$.
473 The growth experiments with opines were repeated five times and the control experiments two
474 (glycerol) to three (sucrose+NH_4) times.

475 **Sequencing and identification of bacterial genomes**

476 Eight bacterial CG isolates (CG1-CG8) were sequenced either using an Illumina Miseq (2014,
477 CG1-CG2 and CG4-CG6, 2x250 bp V2 chemistry) or a NextSeq (2017, CG3 and CG7-CG8,
478 2x150bp mid-throughput v2 500/550 kit) after library preparation with the Nextera XT and 24

bioRxiv preprint doi: https://doi.org/10.1101/2023.06.20.545721; this version posted November 21, 2023. The copyright holder for this preprint (which was not certified by peer review) is the author/funder, who has granted bioRxiv a license to display the preprint in perpetuity. It is made available under aCC-BY 4.0 International license.

indices kits. Raw reads were quality filtered, corrected (Q30), and assembled using SPAdes 3.10.1 (Bankevich et al. 2012). The assembled sequences were screened for bacterial contaminations using blobtools (Laetsch and Blaxter 2017) with taxonomic assignment via BLAST (Altschul et al. 1990). Contigs are assembled DNA-sequences and in this study synonyms of scaffolds and nodes. On the contigs, rRNAs, tRNAs, genes (filtered open reading frames), and coding sequences (CDS) were annotated with PROKKA v1.12 (Seemann 2014) and Barrnap 0.9 (Torsten Seeman, https://github.com/tseemann/barrnap). Completeness of the genomes is indicated by the abundance of the 107 essential genes (Dupont et al. 2012). The overall genome coverage was calculated by mapping the original reads back onto the assembled contigs using Bowtie2 (Langmead and Salzberg 2012). The full length 16S rRNA gene sequences of the *de novo* draft genomes were taxonomically identified with the EZBioCloud database (Yoon et al. 2017). These 16S sequences were also matched with BLAST against the dataset of 16S v4 amplicon sequence variants (ASVs) by Faist et al. 2016 to account for their relative abundances in the whole bacterial community. We calculated a phylogenetic tree using BcgTree (Ankenbrand and Keller 2016), including our *Rhizobiaceae* isolates as well as 94 randomly selected *Rhizobiaceae* bacteria and four *Bradyrhizobium* genomes as an outgroup from EZBioCloud. The accession numbers for the raw reads at NCBI are JABAED000000000, JABAEE000000000, JABAEF000000000, JABAEG000000000, JABAEH000000000, JABAEI000000000, JABAEJ000000000, JABAED000000000 and JABAIN000000000 while for the annotated assemblies it is DOI: 10.5281/zenodo.3752520.

Comparative genomics

A total of 34 reference genomes were used in addition to the eight genomes from this study. The references include 14 strains of *A. vitis*, two strains of *A. fabrum/tumefaciens*, eight strains of *A. rhizogenes*, six strains from the genus *Pseudomonas*, one from *Rahnella*, one from *Shpingomonas*, and two *Curtobacterium* strains. Strain details and accession numbers are listed

bioRxiv preprint doi: https://doi.org/10.1101/2023.06.20.545721; this version posted November 21, 2023. The copyright holder for this preprint (which was not certified by peer review) is the author/funder, who has granted bioRxiv a license to display the preprint in perpetuity. It is made available under aCC-BY 4.0 International license.

in table 1 and supplementary table 1. Most of the *A. tumefaciens*, *A. vitis*, and *A. rhizogenes* references are described in (Weisberg et al. 2020) including a classification of their oncogenic plasmid and opine metabolism capabilities. Orthologous groups (OG) based on amino acid sequences of our isolates (CG1-CG8) and the reference genomes were identified by OrthoFinder (Emms and Kelly 2015). Gene names were transferred from the reference genomes to all genes of the cluster. Protein families including known Ti-plasmid proteins from the references were sorted into the following functional groups: A) virulence, B) plasmid replication and transfer, and C) utilization of opines (table 2). DNA sequences were aligned with lastZ (Harris 2007) and visualized with AliTV (Ankenbrand et al. 2017). For this comparison, two additional, recently described, plasmids were included, namely pTiAg57 and pAtAg67 (Hooykaas et al. 2022). Genes of these two plasmids were assigned to orthogroups by best BLAST hit (Altschul et al., 1990) with e-value below 10^{-12}. For an unsupervised approach, shared and unique OGs of different bacterial species were displayed in UpSetR (Conway et al. 2017). For identification of putative opine clusters, we analysed the genomic neighbourhood of regions, where homologs of both OoxA/NoxA/VoxA and OoxB/NoxB/VoxB genes are found. We selected fragments of 15 kbp downstream and upstream of these genes for direct comparisons. If not indicated otherwise, gene functional descriptions are from the STRING database (https://string-db.org/, March 2019)

Data Availability

The genome sequences obtained in this study have been deposited at NCBI with BioProject accession number PRJNA624984, annotated assemblies are available from Zenodo with doi:10.5281/zenodo.3752520.

bioRxiv preprint doi: https://doi.org/10.1101/2023.06.20.545721; this version posted November 21, 2023. The copyright holder for this preprint (which was not certified by peer review) is the author/funder, who has granted bioRxiv a license to display the preprint in perpetuity. It is made available under aCC-BY 4.0 International license.

Acknowledgements

Special thanks go to Peter Schwappach (Bavarian Regional Office for Viticulture and Horticulture, Veitshoechheim, Germany) for providing grapevine plants and to Ernö Szegedi (Research Institute for Viticulture and Enology, Kecskemét, Hungary) for providing us with the chemical compounds octopine and nopaline. Many thanks go also to our colleagues from the University of Wuerzburg (in particular Gudrun Grimmer for library preparation for genome sequencing) and the Graduate School of Life Sciences from the University of Wuerzburg. We also want to thank Lisa Walther for her work and the data she contributed to this study and acknowledge Anne Müller and Lorenz Hoffmann, who help us to isolate bacteria that were sequenced in this study during their Master thesis (2012) and Diploma thesis (2013) at the University of Wuerzburg, respectively. Finally, we thank Rainer Hedrich (University of Wuerzburg, Germany) for financial support during this study.

Funding information

This work was supported by the Deutsche Forschungsgemeinschaft Graduiertenkolleg (GK1342 “Progress in lipid signaling”; TPs A8 [U. Hentschel] and A5 [R. Deeken]) and by a development grant of the Chamber of Industry and Commerce 2012, Schweinfurt-Wuerzburg, Germany, to U. Hentschel and R. Deeken. The funders had no role in the study design, data collection and interpretation, or decision to submit the work for publication.

Literature Cited

Altschul SF, Gish W, Miller W, Myers EW, Lipman DJ. 1990. Basic local alignment search tool. J Mol Biol 215: 403-410. doi: 10.1016/S0022-2836(05)80360-2

bioRxiv preprint doi: https://doi.org/10.1101/2023.06.20.545721; this version posted November 21, 2023. The copyright holder for this preprint (which was not certified by peer review) is the author/funder, who has granted bioRxiv a license to display the preprint in perpetuity. It is made available under aCC-BY 4.0 International license.

Ankenbrand MJ, Hohlfeld S, Hackl T, Förster F. 2017. AliTV—interactive visualization of whole genome comparisons. PeerJ Computer Science 3: e116. doi: 10.7717/peerj-cs.116

Ankenbrand MJ, Keller A. 2016. bcgTree: automatized phylogenetic tree building from bacterial core genomes. Genome 59: 783-791. doi: 10.1139/gen-2015-0175

Bankevich A, et al. 2012. SPAdes: a new genome assembly algorithm and its applications to single-cell sequencing. J Comput Biol 19: 455-477. doi: 10.1089/cmb.2012.0021

Bien E, Lorenz D, Eichhorn K. (1990) Isolation and characterization of *Agrobacterium tumefaciens* from the German vineregion Rheinpfalz. J Plant Dis Protect 97: 313-322

Bergeron J, Macleod RA, Dion P. 1990. Specificity of octopine uptake by *Rhizobium* and *Pseudomonas* strains. Appl Environ Microbiol. 56(5): 1453-1458. doi: 10.1128/aem.56.5.1453-1458.1990.

Brencic A, Winans SC. 2005. Detection of and response to signals involved in host-microbe interactions by plant-associated bacteria. Microbiol Mol Biol Rev 69: 155-194. doi: 10.1128/MMBR.69.1.155-194.2005

Burr TJ, Katz BH. 1983. Isolation of *Agrobacterium tumefaciens* biovar 3 from grapevine galls and sap, and from vineyard soil. Phytopathol 73: 163-165.

bioRxiv preprint doi: https://doi.org/10.1101/2023.06.20.545721; this version posted November 21, 2023. The copyright holder for this preprint (which was not certified by peer review) is the author/funder, who has granted bioRxiv a license to display the preprint in perpetuity. It is made available under aCC-BY 4.0 International license.

575 Canaday J, Gérad JC, Crouzet P, Otten L. 1992. Organization and functional analysis of three
576 T-DNAs from the vitopine Ti plasmid pTiS4. Mol Gen Genet. 235(2-3):292-303. doi:
577 10.1007/BF00279373. PMID: 1465104.
578
579 Canfield ML, Moore LW. 1991. Isolation and characterization of opine utilizing strains of
580 *Agrobacterium tumefaciens* and fluorescent strains of *Pseudomonas spp*. from rootstocks of
581 Malus. Phytopathol 1(4): 440–443.
582
583 Chandrasekaran M, Lee JM, Ye BM, Jung SM, Kim J. et al. 2019. Isolation and
584 Characterization of Avirulent and Virulent Strains of *Agrobacterium tumefaciens* from Rose
585 Crown Gall in Selected Regions of South Korea. Plants (Basel) 25;8(11): 452. doi:
586 10.3390/plants8110452.
587
588 Chen J, Xie J. 2011. Role and regulation of bacterial LuxR-like regulators. J Cell Biochem 112:
589 2694-2702. Doi: 10.1002/jcb.23219
590
591 Chen F, Guo YB, Wang JH, Li JY, Wang HM. 2007. Biological Control of Grape Crown Gall
592 by *Rahnella aquatilis* HX2. Plant Dis 91: 957-963. doi: 10.1094/PDIS-91-8-0957
593
594 Chilton WS, Petit A, Chilton M-D, Dessaux Y. 2001. Structure and characterization of the
595 crown gall opines heliopine, vitopine and ridéopine. Phytochemistry 58 (1): 137-142, doi:
596 10.1016/S0031-9422(01)00166-2
597

bioRxiv preprint doi: https://doi.org/10.1101/2023.06.20.545721; this version posted November 21, 2023. The copyright holder for this preprint (which was not certified by peer review) is the author/funder, who has granted bioRxiv a license to display the preprint in perpetuity. It is made available under aCC-BY 4.0 International license.

598 Clare BG, Kerr A, Jones DA. 1990. Characteristics of the nopaline catabolic plasmid in
599 *Agrobacterium* strains K84 and K1026 used for biological control of crown gall disease.
600 Plasmid 23: 126-137. doi: 10.1016/0147-619x(90)90031-7
601
602 Conway JR, Lex A, Gehlenborg N. 2017. UpSetR: an R package for the visualization of
603 intersecting sets and their properties. Bioinformatics 33: 2938-2940. doi:
604 10.1093/bioinformatics/btx364
605
606 De Meyer SE, et al. 2016. Symbiotic *Burkholderia* Species Show Diverse Arrangements of
607 nif/fix and nod Genes and Lack Typical High-Affinity Cytochrome cbb3 Oxidase Genes. Mol
608 Plant Microbe Interact 29: 609-619. doi: 10.1094/MPMI-05-16-0091-R
609
610 Deeken R, et al. 2006. An integrated view of gene expression and solute profiles of Arabidopsis
611 tumors: a genome-wide approach. Plant Cell 18: 3617-3634. doi: 10.1105/tpc.106.044743
612
613 Dessaux Y, Petit A, Farrand S, Murphy P 1998. in The Rhizobiaceae: Molecular Biology of
614 Model Plant-Associated Bacteria. Springer, pp. 173–197.
615
616 Dessaux Y, Faure D. 2018. Quorum Sensing and Quorum Quenching in *Agrobacterium*: A
617 "Go/No Go System"? Genes (Basel) 9. doi: 10.3390/genes9040210
618
619 Dupont CL, et al. 2012. Genomic insights to SAR86, an abundant and uncultivated marine
620 bacterial lineage. ISME J 6: 1186-1199. doi: 10.1038/ismej.2011.189
621

bioRxiv preprint doi: https://doi.org/10.1101/2023.06.20.545721; this version posted November 21, 2023. The copyright holder for this preprint (which was not certified by peer review) is the author/funder, who has granted bioRxiv a license to display the preprint in perpetuity. It is made available under aCC-BY 4.0 International license.

622 Ellis JG, Kerr A, Petit A, Tempe J. 1982. Conjugal transfer of nopaline and agropine Ti-
623 plasmids —The role of agrocinopines. Molecular and General Genetics MGG 186: 269-274.
624 doi: 10.1007/bf00331861
625
626 Emms DM, Kelly S. 2015. OrthoFinder: solving fundamental biases in whole genome
627 comparisons dramatically improves orthogroup inference accuracy. Genome Biol 16: 157. doi:
628 10.1186/s13059-015-0721-2
629
630 Eng WWH, Gan HM, Gan HY, Hudson AO, Savka MA. 2015. Whole-genome sequence and
631 annotation of octopine-utilizing *Pseudomonas kilonensis* (previously *P. fluorescens*) strain
632 1855-344. Genome Announc 3(3): e00463-15. doi:10.1128/genomeA.00463-15.
633
634 Escobar MA, Civerolo EL, Summerfelt KR, Dandekar AM. 2001. RNAi-mediated oncogene
635 silencing confers resistance to crown gall tumorigenesis. Proc Natl Acad Sci U S A 98: 13437-
636 13442. doi: 10.1073/pnas.241276898
637
638 Faist H, Keller A, Hentschel U, Deeken R. 2016. Grapevine (Vitis vinifera) Crown Galls Host
639 Distinct Microbiota. Appl Environ Microbiol 82: 5542-5552. doi: 10.1128/AEM.01131-16
640
641 Ferreira JHS, van Zyl FGH, Staphorst JL 1992. *Agrobacterium tumefaciens* biovar 3
642 Responsible for Reduction in Yield and Vigour of Muscat d'Alexandrie. South African J. Enol.
643 Vitic. S AFR J ENOL VITIC 13: 78-80.
644

bioRxiv preprint doi: https://doi.org/10.1101/2023.06.20.545721; this version posted November 21, 2023. The copyright holder for this preprint (which was not certified by peer review) is the author/funder, who has granted bioRxiv a license to display the preprint in perpetuity. It is made available under aCC-BY 4.0 International license.

645 Gan HM, et al. 2019. Insight Into the Microbial Co-occurrence and Diversity of 73 Grapevine
646 (Vitis vinifera) Crown Galls Collected Across the Northern Hemisphere. Front Microbiol 10:
647 1896. doi: 10.3389/fmicb.2019.01896
648
649 Gan HM, Savka MA. 2018. One More Decade of *Agrobacterium* Taxonomy. Curr Top
650 Microbiol Immunol 418:1-14. doi: 10.1007/82_2018_81.
651
652 Gelvin SB. 2010. Plant proteins involved in *Agrobacterium*-mediated genetic transformation.
653 Annu Rev Phytopathol 48: 45-68. doi: 10.1146/annurev-phyto-080508-081852
654
655 Gohlke J, et al. 2013. DNA methylation mediated control of gene expression is critical for
656 development of crown gall tumors. PLoS Genet 9: e1003267. doi:
657 10.1371/journal.pgen.1003267
658
659 Gordon JE, Christie PJ. 2014. The *Agrobacterium* Ti plasmids. Microbiol Spectrum 2(6):
660 PLAS-0010-2013. doi: 10.1128 /microbiolspec.PLAS-0010-2013.
661
662 Harris RS, editor. 2007. Improved pairwise alignment of genomic DNA. The Pennsylvania
663 State University.
664
665 Haudecoeur E, Faure D. 2010. A fine control of quorum-sensing communication in
666 *Agrobacterium tumefaciens*. Commun Integr Biol 3(2): 84-88. doi: 10.4161/cib.3.2.10429.
667

bioRxiv preprint doi: https://doi.org/10.1101/2023.06.20.545721; this version posted November 21, 2023. The copyright holder for this preprint (which was not certified by peer review) is the author/funder, who has granted bioRxiv a license to display the preprint in perpetuity. It is made available under aCC-BY 4.0 International license.

668 Haudecoeur E, et al. 2009. Different regulation and roles of lactonases AiiB and AttM in
669 *Agrobacterium tumefaciens* C58. Mol Plant Microbe Interact 22: 529-537. doi: 10.1094/MPMI-
670 22-5-0529
671
672 Hooykaas M, et al. 2022. Characterization of the Agrobacterium octopine-cucumopine catabolic
673 plasmid pAtAg67. Plasmid 121. doi: 10.1016/j.plasmid.2022.102629
674
675 Klee H, et al. 1984. Nucleotide sequence of the tms genes of the pTiA6NC octopine Ti plasmid:
676 two gene products involved in plant tumorigenesis. Proc Natl Acad Sci U S A 81: 1728-1732.
677 doi: 10.1073/pnas.81.6.1728
678
679 Laetsch D, Blaxter M. 2017. BlobTools: Interrogation of genome assemblies [version 1; peer
680 review: 2 approved with reservations]. F1000Research 6. doi: 10.12688/f1000research.12232.1
681
682 Lang J, et al. 2017. Fitness costs restrict niche expansion by generalist niche-constructing
683 pathogens. ISME J 11: 374-385. doi: 10.1038/ismej.2016.137
684
685 Lang J, Gonzalez-Mula A, Taconnat L, Clement G, Faure D. 2016. The plant GABA signaling
686 downregulates horizontal transfer of the *Agrobacterium tumefaciens* virulence plasmid. New
687 Phytol 210: 974-983. doi: 10.1111/nph.13813
688
689 Lang J, Faure D. 2014. Functions and regulation of quorum-sensing in *Agrobacterium*
690 *tumefaciens*. Front Plant Sci 5: 14. doi: 10.3389/fpls.2014.00014
691

bioRxiv preprint doi: https://doi.org/10.1101/2023.06.20.545721; this version posted November 21, 2023. The copyright holder for this preprint (which was not certified by peer review) is the author/funder, who has granted bioRxiv a license to display the preprint in perpetuity. It is made available under aCC-BY 4.0 International license.

692 Langmead B, Salzberg SL. 2012. Fast gapped-read alignment with Bowtie 2. Nat Methods 9:
693 357-359. doi: 10.1038/nmeth.1923
694
695 Mel SF, Mekalanos JJ. 1996. Modulation of Horizontal Gene Transfer in Pathogenic Bacteria
696 by In Vivo Signals. Cell 87: 795–798. doi: 10.1016/s0092-8674(00)81986-8
697
698 Moore LW, Chilton WS, Canfield ML. 1997. Diversity of opines and opine-catabolizing
699 bacteria isolated from naturally occurring crown gall tumors. Appl Environ Microbiol 63: 201-
700 207. doi: 10.1128/aem.63.1.201-207.1997
701
702 Nautiyal CS, Dion P. 1990. Characterization of the Opine-Utilizing Microflora Associated with
703 Samples of Soil and Plants. Appl Environ Microbiol 56: 2576-2579. doi:
704 10.1128/aem.56.8.2576-2579.1990
705
706 Petit A, et al. 1983. Further extension of the opine concept: Plasmids in *Agrobacterium*
707 *rhizogenes* cooperate for opine degradation. Molecular and General Genetics MGG 190: 204-
708 214. doi: 10.1007/bf00330641
709
710
711 Pitzschke A, Hirt H. 2010. New insights into an old story: *Agrobacterium*-induced tumour
712 formation in plants by plant transformation. EMBO J 29: 1021-1032. doi:
713 10.1038/emboj.2010.8
714

bioRxiv preprint doi: https://doi.org/10.1101/2023.06.20.545721; this version posted November 21, 2023. The copyright holder for this preprint (which was not certified by peer review) is the author/funder, who has granted bioRxiv a license to display the preprint in perpetuity. It is made available under aCC-BY 4.0 International license.

715 Platt TG, Morton ER, Barton IS, Bever JD, Fuqua C. 2014. Ecological dynamics and complex
716 interactions of *Agrobacterium* megaplasmids. Frontiers Plant Sci 5: doi:
717 10.3389/fpls.2014.00635
718
719 Platt TG, Fuqua C, Bever JD. 2012. Resource and competitive dynamics shape the benefits of
720 public goods cooperation in a plant pathogen. Evolution 66: 1953-1965. doi: 10.1111/j.1558-
721 5646.2011.01571.x
722
723 Ryu MH, et al. 2020. Control of nitrogen fixation in bacteria that associate with cereals. Nat
724 Microbiol 5: 314-330. doi: 10.1038/s41564-019-0631-2
725
726 Schrammeijer B, den Dulk-Ras A, Vergunst AC, Jurado Jacome E, Hooykaas PJ. 2003.
727 Analysis of Vir protein translocation from *Agrobacterium tumefaciens* using Saccharomyces
728 cerevisiae as a model: evidence for transport of a novel effector protein VirE3. Nucleic Acids
729 Res 31: 860-868. doi: 10.1093/nar/gkg179
730
731 Schroth M, McCain A, Foott J, Huisman O. 1988. Reduction in yield and vigor of grapevine
732 caused by crown gall disease. Plant Disease 72: 241-246. doi:10.1094/PD-72-0241
733
734 Seemann T. 2014. Prokka: rapid prokaryotic genome annotation. Bioinformatics 30: 2068-
735 2069. doi: 10.1093/bioinformatics/btu153
736
737 Shiraishi A, Matsushita N, Hougetsu T. 2010. Nodulation in black locust by the
738 Gammaproteobacteria *Pseudomonas sp*. and the Betaproteobacteria *Burkholderia sp*. Syst Appl
739 Microbiol 33: 269-274. doi: 10.1016/j.syapm.2010.04.005
740

bioRxiv preprint doi: https://doi.org/10.1101/2023.06.20.545721; this version posted November 21, 2023. The copyright holder for this preprint (which was not certified by peer review) is the author/funder, who has granted bioRxiv a license to display the preprint in perpetuity. It is made available under aCC-BY 4.0 International license.

741 Slater SC, et al. 2009. Genome sequences of three agrobacterium biovars help elucidate the
742 evolution of multichromosome genomes in bacteria. J Bacteriol. 191(8):2501-11. doi:
743 10.1128/JB.01779-08

744

745 Subramoni S, Nathoo N, Klimov E, Yuan ZC. 2014. *Agrobacterium tumefaciens* responses to
746 plant-derived signaling molecules. Front Plant Sci 5: 322. doi: 10.3389/fpls.2014.00322

747

748 Szegedi E. 2003 Opines in naturally infected grapevine crown gall tumors. Vitis 42 (1): 39–41,
749 doi: 10.5073/vitis.2003.42.39-41

750

751 Szegedi E, Czako M, Otten L. 1996. Further evidence that the vitopine-type pTi's of
752 *Agrobacterium vitis* represent a novel group of Ti plasmids. Mol Plant Microbe Interact 9: 139-
753 143. doi: 10.1094/MPMI-9-0139

754

755 Szegedi E, Czakó M, Koncz CS. 1988. Opines in crown gall tumours induced by biotype 3
756 isolates of *Agrobacterium tumefaciens*. Physiol Mol Plant Pathol 3(5): 237-247, doi:
757 10.1016/S0885-5765(88)80020-1

758

759 Vergunst AC, et al. 2005. Positive charge is an important feature of the C-terminal transport
760 signal of the VirB/D4-translocated proteins of *Agrobacterium*. Proc Natl Acad Sci USA 102:
761 832–837. doi: 10.1073/pnas.0406241102.

762

bioRxiv preprint doi: https://doi.org/10.1101/2023.06.20.545721; this version posted November 21, 2023. The copyright holder for this preprint (which was not certified by peer review) is the author/funder, who has granted bioRxiv a license to display the preprint in perpetuity. It is made available under aCC-BY 4.0 International license.

763 Vladimirov IA, Matveeva TV, Lutova LA. 2015. Opine biosynthesis and catabolism genes of
764 *Agrobacterium* tumefaciens and *Agrobacterium rhizogenes*. Russ J Genet 51: 121–129. doi:
765 10.1134/S1022795415020167

766

767 Vigouroux A, et al. 2017. Structural basis for high specificity of octopine binding in the plant
768 pathogen *Agrobacterium tumefaciens.* Sci Rep 7: 18033. doi: 10.1038/s41598-017-18243-8

769

770 Weisberg A, et al. 2020. Unexpected conservation and global transmission of agrobacterial
771 virulence plasmids. Science. 368. eaba5256. 10.1126/science.aba5256. doi:
772 10.1126/science.aba5256.

773

774 Wetzel ME, Kim KS, Miller M, Olsen GJ, Farrand SK. 2014. Quorum-dependent mannopine-
775 inducible conjugative transfer of an *Agrobacterium* opine-catabolic plasmid. J Bacteriol 196:
776 1031-1044. doi: 10.1128/JB.01365-13

777

778 Wikipedia contributors. 2023. Ti plasmid. In: Wikipedia, The Free Encyclopedia. Retrieved
779 from https://en.wikipedia.org/w/index.php?title=Ti_plasmid&oldid=1144023521

780

781 Winans SC, Ebert PR, Stachel SE, Gordon MP, Nester EW. 1986. A gene essential for
782 *Agrobacterium* virulence is homologous to a family of positive regulatory loci. Proc Natl Acad
783 Sci U S A 83: 8278-8282. doi: 10.1073/pnas.83.21.8278

784

785 Wise AA, Binns AN. 2015. The Receiver of the *Agrobacterium tumefaciens* VirA Histidine
786 Kinase Forms a Stable Interaction with VirG to Activate Virulence Gene Expression. Front
787 Microbiol 6: 1546. doi: 10.3389/fmicb.2015.01546

bioRxiv preprint doi: https://doi.org/10.1101/2023.06.20.545721; this version posted November 21, 2023. The copyright holder for this preprint (which was not certified by peer review) is the author/funder, who has granted bioRxiv a license to display the preprint in perpetuity. It is made available under aCC-BY 4.0 International license.

Yoon SH, et al. 2017. Introducing EzBioCloud: a taxonomically united database of 16S rRNA gene sequences and whole-genome assemblies. Int J Syst Evol Microbiol 67: 1613-1617. doi: 10.1099/ijsem.0.001755

Zanker H, von Lintig J, Schröder J. 1992. Opine transport genes in the octopine (occ) and nopaline (noc) catabolic regions in Ti plasmids of *Agrobacterium tumefaciens*. J Bacteriol. 174(3):841-9. doi: 10.1128/jb.174.3.841-849.1992.

Zanker H, et al. 1994. Octopine and nopaline oxidases from Ti plasmids of *Agrobacterium tumefaciens*: molecular analysis, relationship, and functional characterization. J Bacteriol 176: 4511-4517. doi: 10.1128/jb.176.15.4511-4517.1994

bioRxiv preprint doi: https://doi.org/10.1101/2023.06.20.545721; this version posted November 21, 2023. The copyright holder for this preprint (which was not certified by peer review) is the author/funder, who has granted bioRxiv a license to display the preprint in perpetuity. It is made available under aCC-BY 4.0 International license.

801

Figure 1

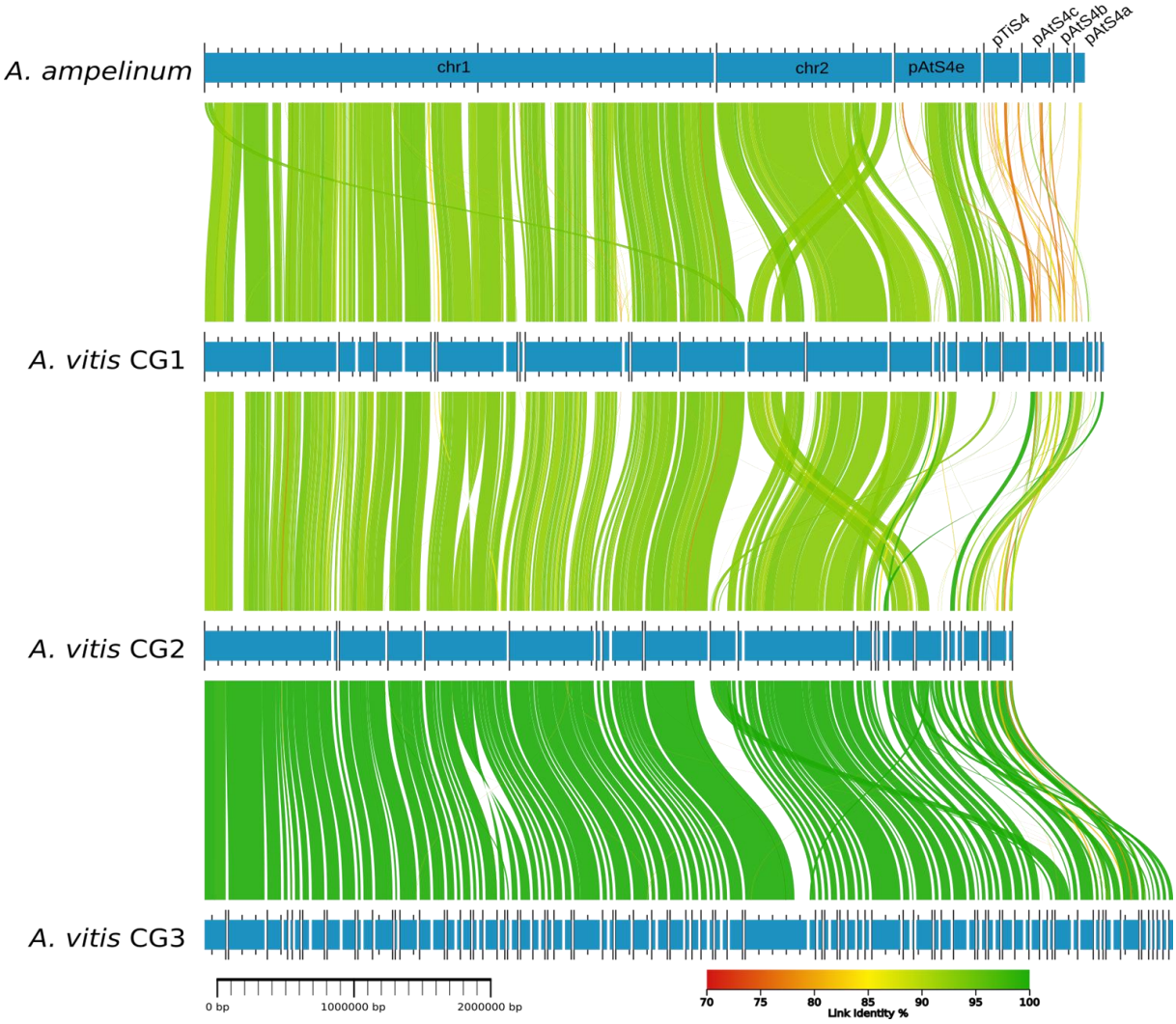

802

803 **Fig. 1** DNA alignment of *Allorhizobium vitis* genomes. Blue horizontal bars indicate the
804 chromosomes (chr1, chr2) and plasmids (pATS4e, pTiS4, pTiS4a-c) of *A. ampelinum*, and the
805 contigs of the *A. vitis* CG1-CG3 genome sequences. Homologous regions between genomes are
806 connected via lines of different colors. A color gradient (70 to 100%) according to the similarity
807 (Link identity %) is provided.

808

bioRxiv preprint doi: https://doi.org/10.1101/2023.06.20.545721; this version posted November 21, 2023. The copyright holder for this preprint (which was not certified by peer review) is the author/funder, who has granted bioRxiv a license to display the preprint in perpetuity. It is made available under aCC-BY 4.0 International license.

809 **Figure 2**

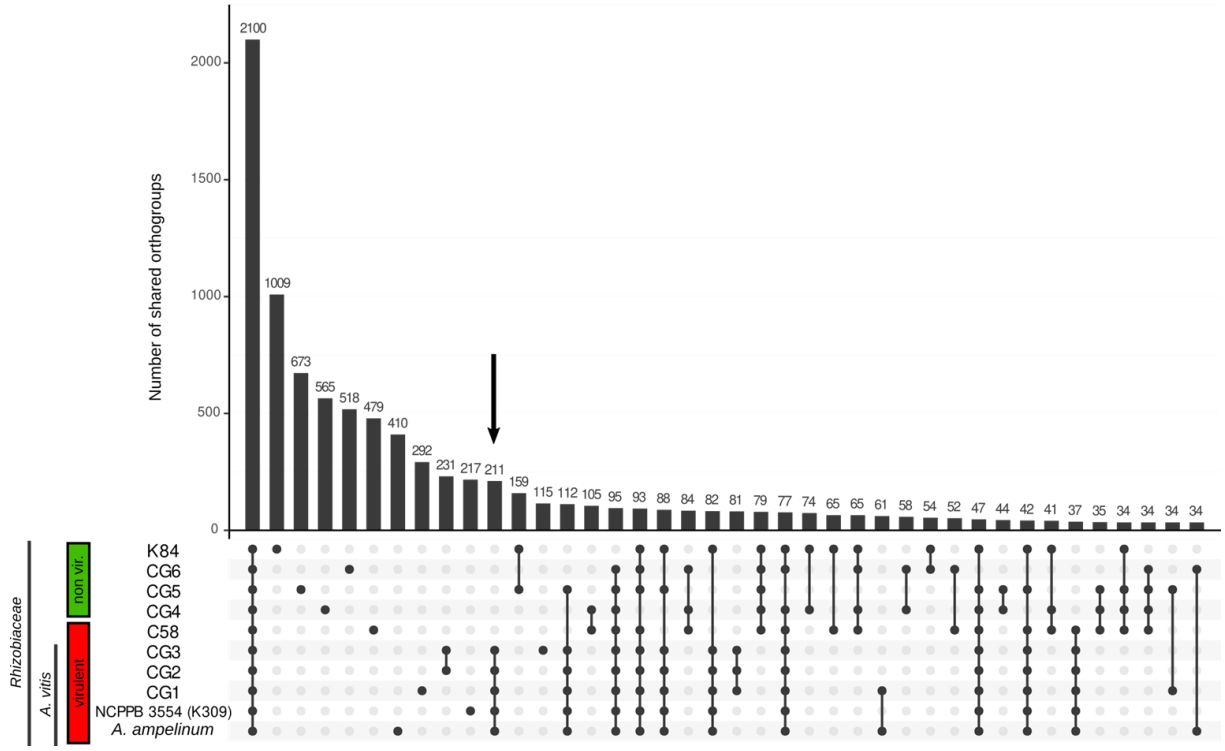

810

811 **Fig. 2.** Shared and unique orthologous groups encoded by the sequences of the *Rhizobiaceae*
812 genomes (CG1-CG6) and the references *A. ampelinum*, *A. vitis* NCPPB3554 (K309), *A. fabrum*
813 C58, and *A. rhizogenes* K84. Each column represents the number of orthologous genes only
814 shared by the genomes (black dots below each bar). The red box indicates virulent bacteria and
815 the green box non-virulent. Less than 34 shared protein families are not shown.

816

bioRxiv preprint doi: https://doi.org/10.1101/2023.06.20.545721; this version posted November 21, 2023. The copyright holder for this preprint (which was not certified by peer review) is the author/funder, who has granted bioRxiv a license to display the preprint in perpetuity. It is made available under aCC-BY 4.0 International license.

817 **Figure 3**

818

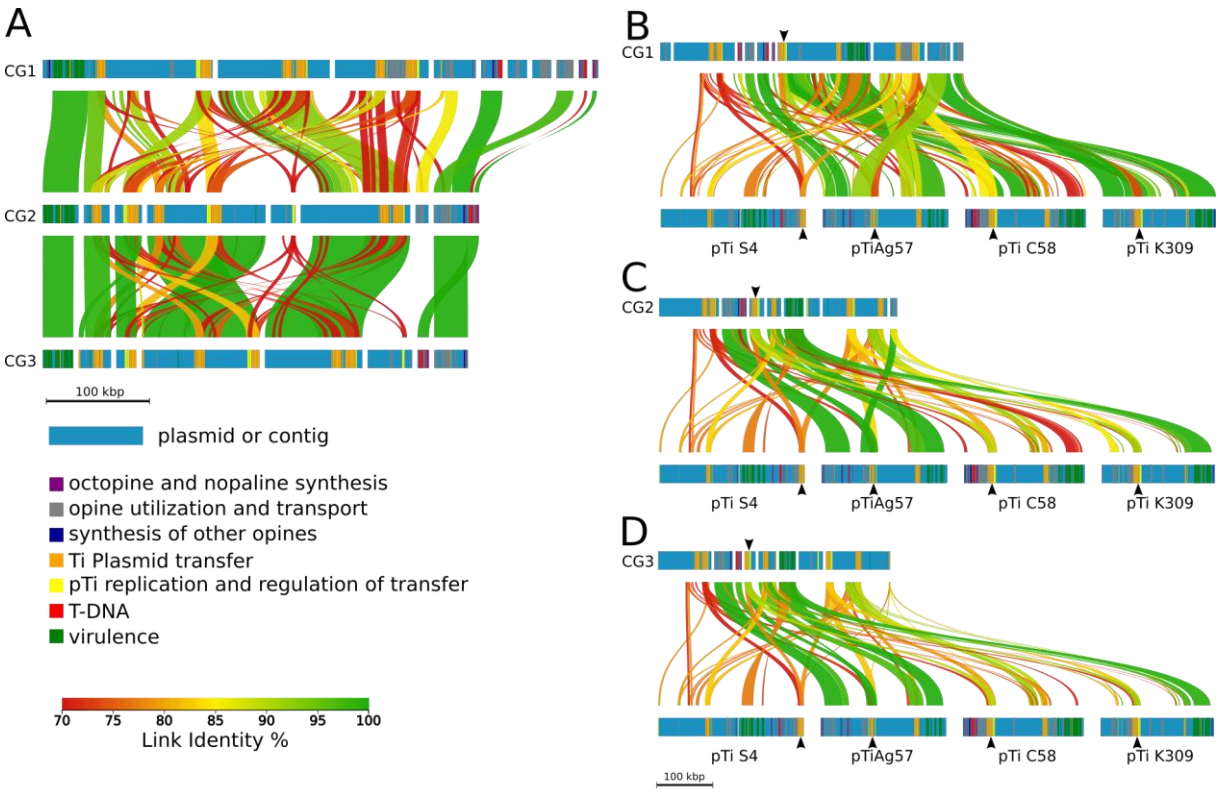

819 **Fig. 3.** DNA alignments of Ti plasmid regions of the *de novo* sequenced isolates CG1-CG3 and
820 three reference pTis. **(A)** Alignment of CG1, CG2, and CG3 and **(B-D)** of potential Ti-plasmids
821 from CG1-CG3 to the reference Ti-plasmids of *A. ampelinum* (vitopine/heliopine-type), *A.*
822 *fabrum* Ag57 (octopine/cucumopine-type), *A. fabrum* C58 (nopaline-type), and *A. vitis*
823 NCPPB3554 (pTiK309) (octopine/cucumopine-type). Colored horizontal bars represent
824 contigs of the potential Ti-plasmids and reference pTis. The position of predicted protein
825 functions is marked by different colors. Homologous regions between the contigs are connected
826 via vertical-colored lines and the color gradient shows % similarity (Link Identity %). Black
827 arrow heads indicate the regions for Ti plasmid transfer (orange bars) and pTi plasmid
828 replication (yellow bars) with highest homology to the reference plasmids.

829

bioRxiv preprint doi: https://doi.org/10.1101/2023.06.20.545721; this version posted November 21, 2023. The copyright holder for this preprint (which was not certified by peer review) is the author/funder, who has granted bioRxiv a license to display the preprint in perpetuity. It is made available under aCC-BY 4.0 International license.

830 **Figure 4**

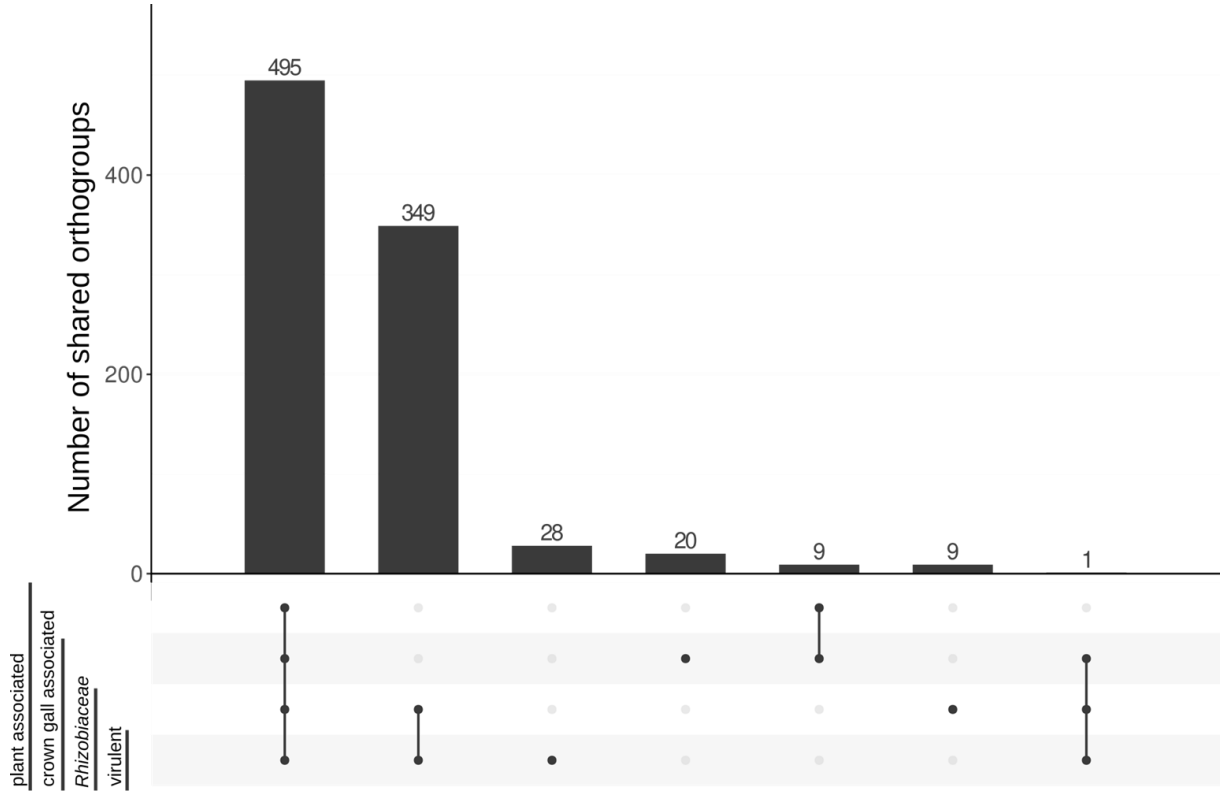

831

832 **Fig. 4.** Shared and unique protein families among the selected genomes. These are grouped into
833 i) plant associated, ii) crown gall associated, iii) Rhizobiaceae, and iv) virulent. The four groups
834 consist of the following members i) *Pseudomonas cerasi*, *Rhanella aquatilis*, *Shpingomonas*
835 *sp*. Leaf230, *Curtobacterium strain 6*, *Curtobacterium flaccumfaciens,* ii) *Pseudomonas* CG7
836 and *Rhanella* CG8, iii) non-virulent *Rhizobiaceae CG4-CG6,* and iv) *Agrobacterium fabrum*
837 *C58, Allorhizobium ampelinum,* the virulent *Allorhizobium vitis* isolates C*G1-CG3*. A protein
838 family is part of a group if it occurs in all members (black dots). A protein family is not part of
839 a group if it occurs in none of the members. Protein families that occur in some representatives
840 of a group are discarded.

841

bioRxiv preprint doi: https://doi.org/10.1101/2023.06.20.545721; this version posted November 21, 2023. The copyright holder for this preprint (which was not certified by peer review) is the author/funder, who has granted bioRxiv a license to display the preprint in perpetuity. It is made available under aCC-BY 4.0 International license.

842 **Figure 5**

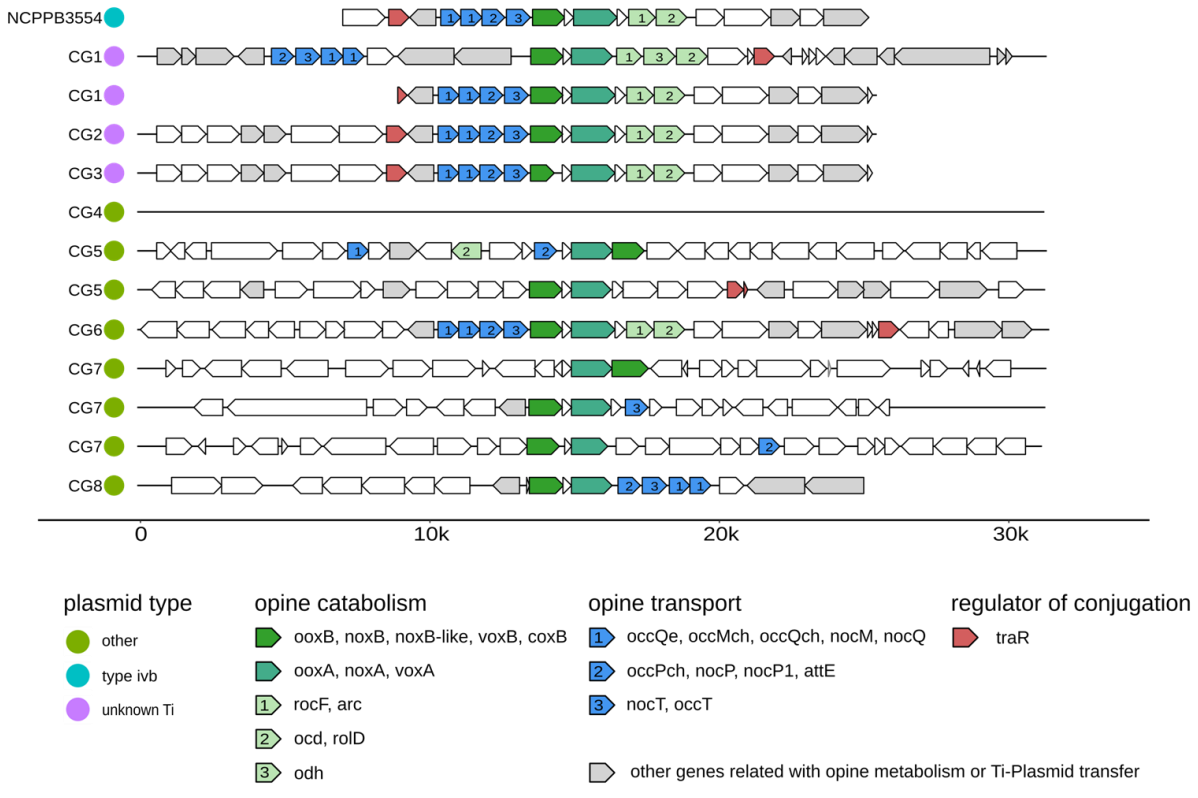

843

844 **Fig. 5.** Regions in the *de novo* sequenced genomes of the CG1-CG8 isolates from grapevine
845 crown galls that contain orthologs to both ooxA and ooxB, compared to the octopine catabolism
846 cluster of pAtK309. The horizontal black lines represent a part of a contig centered around the
847 ooxA/B, noxA/B, voxA/B genes. Colored arrows symbolize the orientation of coding regions
848 including known annotations of PROKKA. Green colors symbolize opine catabolism; blue,
849 opine transport; red, regulator of plasmid conjugation, and grey, other genes related with opine
850 metabolism or Ti-plasmid transfer. The number within the arrows specify the gene function
851 within a cluster.

bioRxiv preprint doi: https://doi.org/10.1101/2023.06.20.545721; this version posted November 21, 2023. The copyright holder for this preprint (which was not certified by peer review) is the author/funder, who has granted bioRxiv a license to display the preprint in perpetuity. It is made available under aCC-BY 4.0 International license.

852 **Figure 6**

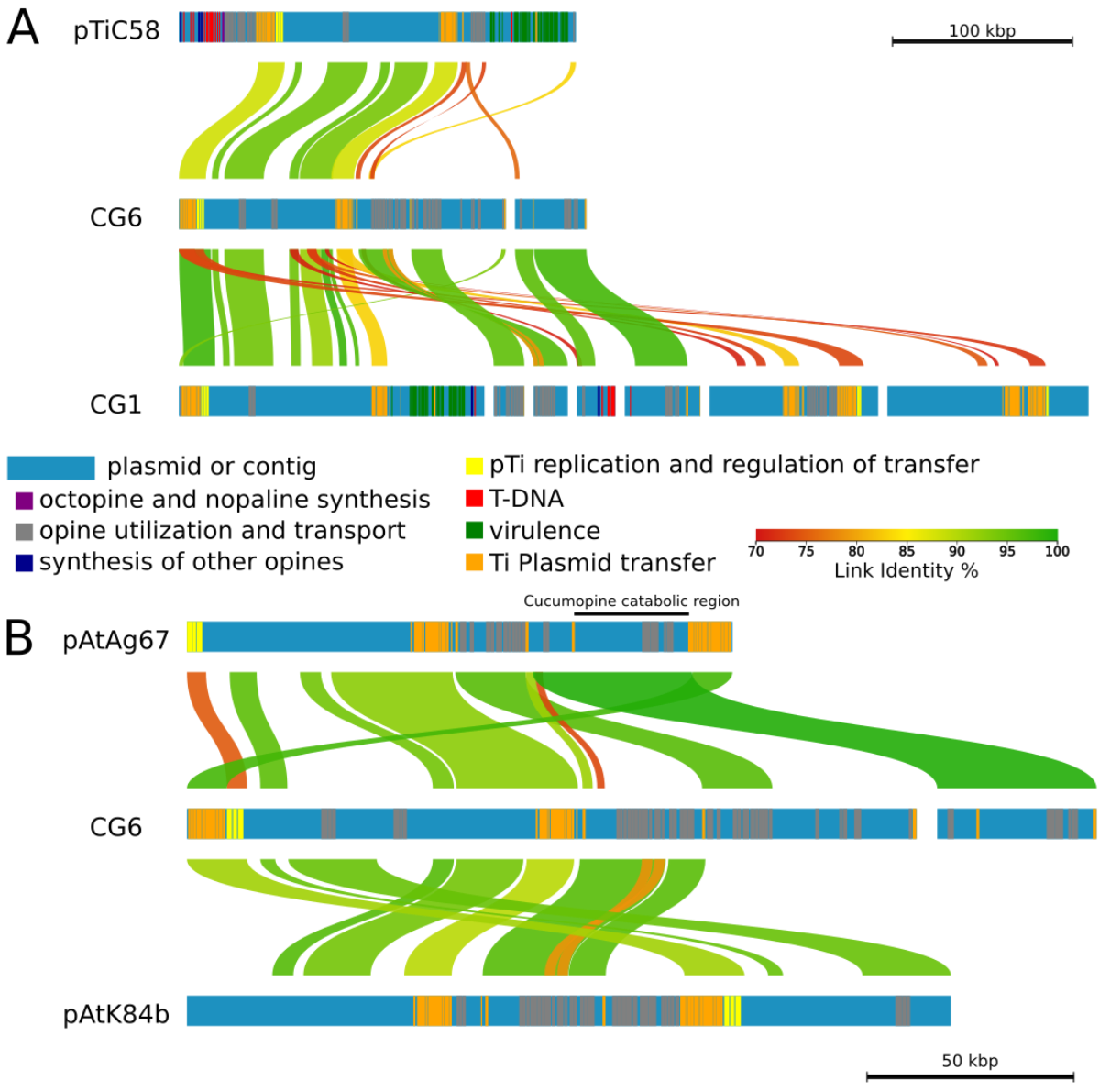

853

854 **Fig. 6.** DNA alignment of putative plasmid sequences with reference plasmids. Colored
855 horizontal bars represent the contigs and encoded protein families colored according to their
856 function. Homologous regions between the sequences are connected via lines in a color gradient
857 corresponding to % similarity (Link Identity %). **(A)** alignment of pTi regions from the
858 reference strain *A. fabrum C58* and putative plasmid sequences of two isolates, the virulent *A.*
859 *vitis* CG1 and non-virulent *A. rosae* CG6. **(B)** alignment of the opine-catabolic plasmid regions
860 from the virulent reference *A. fabrum* Ag57 (pAtAg67), the non-virulent

bioRxiv preprint doi: https://doi.org/10.1101/2023.06.20.545721; this version posted November 21, 2023. The copyright holder for this preprint (which was not certified by peer review) is the author/funder, who has granted bioRxiv a license to display the preprint in perpetuity. It is made available under aCC-BY 4.0 International license.

agrocinopine/nopaline-type plasmid of *A. rhizogenes K84* (pAtK84b) and putative plasmid sequences of the non-virulent *A. rosae* CG6. The cucumopine catabolic region of pAtAg67, according to Hooykaas et al. (2022) is indicated with a black bar.

bioRxiv preprint doi: https://doi.org/10.1101/2023.06.20.545721; this version posted November 21, 2023. The copyright holder for this preprint (which was not certified by peer review) is the author/funder, who has granted bioRxiv a license to display the preprint in perpetuity. It is made available under aCC-BY 4.0 International license.

Table 1. Information about the bacterial genomes analysed in this study (1.-3., 7.-11.) and the known reference sequences (4.-6., 12.-16.) used for comparison. The selection criteria for the sequences were: i) 'enrichment' or 'reduction' of the 16S rRNA V4 amplicon sequences in crown galls in springtime (Faist et al., 2016), ii) member of the *Rhizobiaceae* family, (iii) part of the agrobacterial virulence plasmid study Weisberg et al., 2020, iv) endophytic in grapevine graft unions without crown gall disease, and v) biocontrol for crown gall disease. Annotation statistics for genomes from this study or according to NCBI assembly report (genome annotation data, if available, indicated with *), CDS, coding sequences

	Name* (database accession number and/or reference)	Selection criteria	Predicted CDS	tRNAs, rRNAs	Essential genes (Completeness), Missing genes
	Virulent Rhizobiaceae				
1.	*A. vitis CG1*, this study	*Rhizobiaceae*, enrichment	5,727	56, 12	106 (99.1%), TIGR01030 (rpmH)
2.	*A. vitis CG2*, this study	*Rhizobiaceae*, enrichment	5,051	49, 3	106 (99.1%), TIGR01030 (rpmH)
3.	*A. vitis CG3*, this study	*Rhizobiaceae*, enrichment	5,550	50, 3	106 (99.1%), TIGR01030 (rpmH)
4.	*A. vitis S4* (Slater et al. 2009, CP000637.1)	Weisberg et al.	5,729 *	55, 12*	
5.	*A. fabrum C58* (Goodner et al. 2001, Wood et al. 2001, SAMN02603108)	Weisberg et al.	5,253*	53, 12*	
6.	*A. rhizogenes K84 (SAMN02602977)*	Weisberg et al.	6,836*	52, 9*	
7.	*A. vitis NCPPB3554 (K309) (SAMN04223557)*	Weisberg et al.	na	na	
8.	*A. rhizogenes CG101/95 (SAMN14165425)*	Weisberg et al.	6,185*	49, 3*	
9.	*A. rhizogenes CM79/95 (SAMN14165429)*	Weisberg et al.	6,931*	48, 3*	
10.	*A. vitis BM37/95 (SAMN14165430)*	Weisberg et al.	5,398*	49, 2*	
11.	*A. vitis P86/93 (SAMN14165436)*	Weisberg et al.	5,392*	50, 3*	
12.	*A. vitis T268/95 (SAMN14165437)*	Weisberg et al.	5,497*	49, 3*	
13.	*A. vitis T60/94 (SAMN14165442)*	Weisberg et al.	5,509*	50, 3*	

bioRxiv preprint doi: https://doi.org/10.1101/2023.06.20.545721; this version posted November 21, 2023. The copyright holder for this preprint (which was not certified by peer review) is the author/funder, who has granted bioRxiv a license to display the preprint in perpetuity. It is made available under aCC-BY 4.0 International license.

14.	*A. rhizogenes U167/95 (SAMN14165443)*	Weisberg et al.	6,205*	47, 2*	
15.	*A. rhizogenes D1/94 (SAMN14165450)*	Weisberg et al.	6,692*	48, 3*	
16.	*A. vitis T267/94 (SAMN14165455)*	Weisberg et al.	5,458*	50, 3*	
17.	*A. vitis T393/94 (SAMN14165459)*	Weisberg et al.	5,069*	50, 2*	
18.	*A. vitis V80/94 (SAMN14165463)*	Weisberg et al.	5,359*	49, 2*	
19.	*A. vitis AV25/95 (SAMN14165468)*	Weisberg et al.	5,255*	50, 2*	
20.	*A. rhizogenes CM65/95 (SAMN14165470)*	Weisberg et al.	6,554*	48, 3*	
21.	*A. tumefaciens CG53/95 (SAMN14165473)*	Weisberg et al.	5,469*	51, 3*	
22.	*A. rhizogenes T155/95 (SAMN14165487)*	Weisberg et al.	6,240*	47, 3*	
23.	*A. rhizogenes CM80/95 (SAMN14165490)*	Weisberg et al.	6,939*	48, 2*	
24.	*A. vitis CG412 (SAMN14165504)*	Weisberg et al.	4,706*	50, 6*	
25.	*A. vitis CG678 (SAMN14165505)*	Weisberg et al.	5,332*	45, 3*	
26.	*A. vitis CG78 (SAMN14165506)*	Weisberg et al.	5,332*	45, 3*	
27.	*A. vitis F2/5 (SAMN14165507)*	Weisberg et al.	5,251*	48, 3*	
	Non-virulent Rhizobiaceae				
28.	*A. divergens CG4*, this study	*Rhizobiaceae*	5,470	48, 3	106 (99.1%), TIGR01030 (rpmH)
29.	*Rhizobiaceae sp. CG5*, this study	*Rhizobiaceae*	6,251	46, 3	105 (98.1%), TIGR00631 (uvrB), TIGR01030 (rpmH)
30.	*A. rosae CG6*, this study	*Rhizobiaceae*	5,569	51, 6	107 (100%), TIGR01030 (rpmH)
	Other Proteobacteria				
31.	*Pseudomonas sp. CG7*, this study	enrichment	6,002	69, 4	103 (96.3%), TIGR00810 (secG), TIGR02432 (tilS), TIGR03594 (engA), TIGR01030 (rpmH)
32.	*Rahnella sp. CG8*, this study	enrichment	5,099	71, 4	No missing genes
33.	*Pseudomonas cerasi* (Kaluzna et al. 2016, SAMEA3894894)	enrichment	5,725*	63, 15*	
34.	*Rahnella aquatilis* HX2	biocontrol	5,127*	76, 22*	

bioRxiv preprint doi: https://doi.org/10.1101/2023.06.20.545721; this version posted November 21, 2023. The copyright holder for this preprint (which was not certified by peer review) is the author/funder, who has granted bioRxiv a license to display the preprint in perpetuity. It is made available under aCC-BY 4.0 International license.

	(Guo et al. 2012, SAMN02603118)				
35.	*Sphingomonas* sp. Leaf230 (SAMN04151690)	reduction	3,613*	51, 3*	
36.	*Pseudomonas congelans H346-M (SAMN15924736)*	enrichment	4,944*	57, 3*	
37.	*P. savastanoi pv. Glycinea (SAMN03976351)*	enrichment	na	na	
38.	*P. avellanae (SAMN05861163)*	enrichment	5,782*	56, 4*	
39.	*P. sp. 18058 (SAMEA6372291)*	enrichment	na	na	
40.	*P. koreensis Cl12 (SAMN06018396)*	enrichment	5,792*	70, 15*	
	Actinobacteria				
41.	*Curtobacterium flaccumfaciens* MCBA15_005 (SAMN05736482)	reduction	3,465*	45, 4*	
42.	*Curtobacterium sp.* strain 6 (Bulgari et al. 2014, SAMN02709057)	endophytic	na	na	

873
874

bioRxiv preprint doi: https://doi.org/10.1101/2023.06.20.545721; this version posted November 21, 2023. The copyright holder for this preprint (which was not certified by peer review) is the author/funder, who has granted bioRxiv a license to display the preprint in perpetuity. It is made available under aCC-BY 4.0 International license.

	crown gall-associated											
	Rhizobium, Agrobacterium											
	virulent											
nopaline-catabolism	-	-	-	+	-	-	-	-	-	-	-	-
vitopine/heliopine-catabolism	-	-	-	-	+	-	-	-	-	-	-	-
octopine/cucumopine catabolism	+	+	+	-	-	+	+	-	+	+	+	-
pTi type				Ia	V	IVb						
Predicted function	CG1	CG2	CG3	pTi C58	pTi S4	pTi K309	pTiAg57	CG4	CG5	CG6	CG7	CG8
A) Virulence												
sensory response system detecting wounded plants												
virA	3	2	2	3	3	3	3	5	2	5	4	0
virG	5	6	5	4	6	5	1	5	5	4	11	6
protein complex for T-DNA injection												
virB1	1	1	1	2	1	1	1	1	0	0	0	0
virB2	1	1	1	2	1	1	1	1	0	0	0	0
virB3	1	1	1	2	1	1	1	1	0	0	0	0
virB4	1	1	1	2	2	1	1	1	0	0	0	0
virB5	1	1	1	1	1	1	1	0	0	0	0	0
virB6	1	1	1	1	1	1	1	0	0	0	0	0
virB7, virB8, virB9	0	0	0	1	1	1	1	0	0	0	0	0
virB10	1	1	1	2	2	1	1	0	0	0	0	0
virC1	1	1	1	1	2	1	1	0	0	0	0	0
virC2	1	1	1	1	1	1	1	0	0	0	0	0
virD4	3	2	3	2	3	3	1	0	1	1	0	0
translocated vir-proteins												
virD2	1	1	1	1	1	1	1	0	0	0	0	0
virD5	1	1	1	1	1	1	3	0	0	0	0	0
virE2	1	1	1	1	1	1	1	0	0	0	0	0
virE3	1	1	2	1	1	1	2	0	0	0	0	0
VirF	1	1	1	1	0	1	1	0	0	0	0	0
other vir-genes												
virD1	1	1	1	1	1	1	1	0	0	0	0	0
virD3	0	0	0	1	0	0	0	0	0	0	0	0
virE0	0	0	0	1	0	0	0	0	0	0	0	0
virE1	1	1	1	1	1	1	1	0	0	0	0	0
virH1	1	1	0	1	1	1	1	2	0	0	0	0
virH2	0	0	0	1	0	0	0	0	0	0	1	0
virK	0	0	0	1	1	0	0	0	0	0	0	0
T-DNA onkogenes												
tms2	1	1	1	0	1	1	0	2	4	0	1	0
tms2, iaaM	1	1	1	1	1	3	0	0	0	0	1	0
tms1, iaaH	2	1	1	1	1	2	1	0	0	0	1	0
ipt	2	1	1	2	1	2	1	0	0	0	0	0
other T-DNA genes												
5gene	3	2	2	3	0	2	2	0	0	0	0	0
rolB	0	0	0	1	1	0	0	0	0	0	0	0
6a	1	0	0	1	0	1	1	0	0	0	0	0
6b	1	1	1	1	1	1	1	0	0	0	0	0
B) Plasmid replication and transfer												
repA	5	5	7	3	7	3	1	4	4	4	0	0
repB	4	4	5	3	5	3	1	3	2	4	0	0
repC	1	2	2	1	1	1	1	0	0	1	0	0
traA	3	3	3	3	7	1	1	1	3	5	0	1
traB	3	3	3	1	4	0	1	1	3	3	0	0
traC	3	3	3	2	5	1	1	1	3	3	0	0
traD	3	3	3	2	5	1	1	1	3	3	0	0
traF	5	4	4	1	5	2	1	1	3	3	0	0
traG	3	3	3	2	4	1	1	1	3	3	0	0
traH	3	3	3	1	4	1	1	2	3	3	0	0
traI	2	3	2	1	2	1	1	1	2	3	0	0
traM	3	3	4	1	2	1	1	1	3	3	0	0
traR	5	4	4	1	3	2	2	1	5	5	0	0
trbB, virB11	7	6	6	4	6	5	2	2	5	4	1	0
trbC	3	3	3	1	3	1	1	1	3	3	0	0
trbD	3	3	3	1	3	1	1	1	3	3	0	0
trbE	5	4	4	1	3	3	1	1	4	3	0	0
trbF	3	3	3	1	3	1	1	1	3	3	0	0
trbG	3	3	2	1	3	1	1	1	3	3	0	0
trbH	3	3	3	1	3	1	1	1	3	3	0	0
trbI	5	4	4	1	3	3	1	1	4	4	0	0
trbJ	3	3	3	1	3	1	1	1	3	3	0	0
trbK	2	2	1	1	2	1	1	0	1	3	0	0
trbL	3	3	3	1	3	1	1	1	3	3	0	0
yci	3	4	4	2	4	1	1	3	4	4	0	0

	crown gall-associated											
	Rhizobium, Agrobacterium											
	virulent											
nopaline-catabolism	-	-	-	+	-	-	-	-	-	-	-	-
vitopine/heliopine-catabolism	-	-	-	-	+	-	-	-	-	-	-	-
octopine/cucumopine catabolism	+	+	+	-	-	+	+	-	+	+	+	-
pTi type				Ia	V	IVb						
Predicted function	CG1	CG2	CG3	pTi C58	pTi S4	pTi K309	pTiAg57	CG4	CG5	CG6	CG7	CG8
C) Utilization of opines												
transport												
accA	3	0	0	1	1	1	0	0	4	6	0	0
accB	1	0	0	0	0	1	0	0	0	1	0	0
accC	33	29	37	38	43	34	2	39	46	49	7	34
accD	17	13	17	21	22	17	1	25	28	32	3	21
accE	15	10	16	18	20	15	0	19	24	28	2	18
nocT, occT	4	3	5	4	4	3	1	4	4	5	8	11
occPch, nocP, nocP1, attE	18	14	18	22	16	18	2	20	24	24	21	23
occQe, occMch, occQch, nocM, nocQ	17	13	15	19	14	19	3	18	17	20	21	20
sensing												
nocR	3	1	1	3	4	1	1	7	10	6	5	5
accR	3	0	1	2	2	3	0	1	2	2	1	7
anabolism												
nos, nos-like	0	0	0	1	1	0	0	0	0	0	0	0
vis, cus, ocs	2	2	2	0	2	2	3	0	0	0	0	0
mas1	0	0	0	1	0	0	0	0	0	0	0	0
acs, acsx	2	1	2	2	0	2	3	0	0	0	0	0
catabolism												
ooxA, noxA, voxA	2	1	1	1	3	2	1	1	2	2	4	1
ooxB, noxB, noxB-like, voxB, coxB	2	1	1	1	3	1	1	0	2	1	3	1
rocF, arc	3	2	2	2	1	2	1	1	1	2	0	0
ocd, rolD	5	3	4	3	3	3	1	2	4	3	4	1
odh	1	0	0	2	0	0	0	1	2	0	0	0
accF	4	2	2	3	2	4	1	0	3	4	3	3
accG	3	1	1	4	1	2	1	4	2	3	0	2
hyuA	4	2	4	1	6	3	2	2	4	4	0	1
hyuB	4	2	4	1	6	3	1	2	3	4	0	1
GABA sensing												
blcA	11	12	22	12	16	17	0	11	21	11	28	6
blcB	2	2	2	4	2	2	0	2	2	2	3	2
attM, blcC, aiiB	1	0	0	2	0	1	0	0	0	1	1	0
blcR	0	0	0	1	0	0	0	0	0	0	0	0
bra	2	2	2	3	2	2	0	3	3	3	2	3

Table 2. Number of predicted protein families encoded by the Ti plasmids of the reference bacterial strains *Agrobacterium fabrum* C58 (pTiC85) and LBA649 (pTiAg57), *Allorhizobium ampelinum* (pTiS4), *Allorhizobium vitis* NCPPB3554 (K309), and *A. fabrum* Ag57 (pTiAg57) as well as the de novo sequenced draft genomes of the crown gall associated isolates CG1-CG8. GABA sensing genes are encoded on pAtC58 (NC_003064). Representative names of the predicted protein families are listed in the first column. Gene counts are from whole genome, not only from plasmids, except for pTiAg57 where only the plasmid sequence is known.

bioRxiv preprint doi: https://doi.org/10.1101/2023.06.20.545721; this version posted November 21, 2023. The copyright holder for this preprint (which was not certified by peer review) is the author/funder, who has granted bioRxiv a license to display the preprint in perpetuity. It is made available under aCC-BY 4.0 International license.

877 **Supplementary Material**

878 **Supplementary Fig. 1**

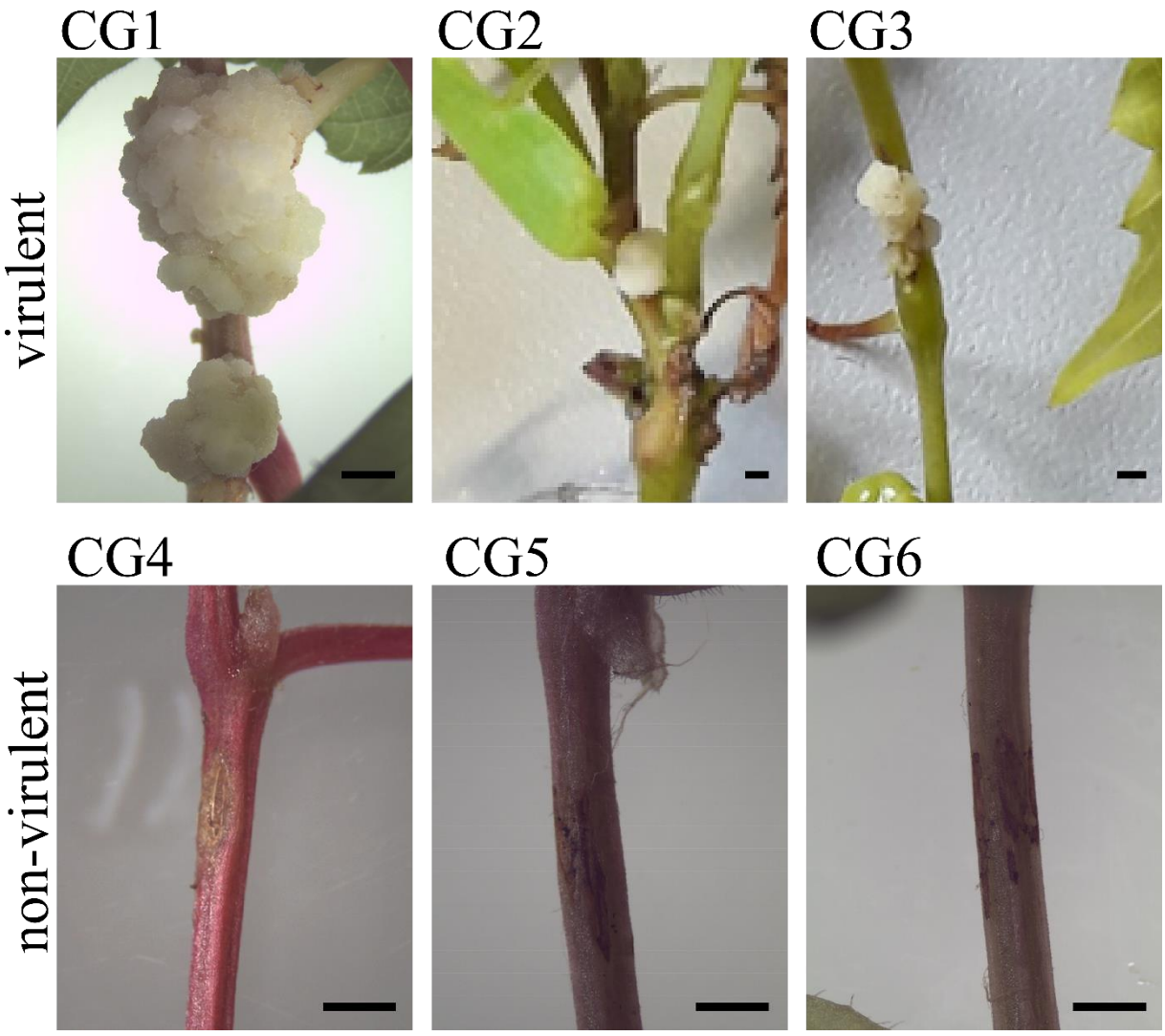

879

880 **Supplementary Fig. 1.** Virulence assay with the bacterial isolates CG1-CG6 and grapevine
881 seedlings. Upper panel: Inoculation of the virulent isolates (CG1-CG3) caused crown gall
882 formation in grapevine stems. Lower panel: Inoculation of the non-virulent isolates (CG4-CG6)
883 induced no crown gall development at the wounded areas of grapevine stems (arrows). Bars
884 represent 0.5 cm.

885

bioRxiv preprint doi: https://doi.org/10.1101/2023.06.20.545721; this version posted November 21, 2023. The copyright holder for this preprint (which was not certified by peer review) is the author/funder, who has granted bioRxiv a license to display the preprint in perpetuity. It is made available under aCC-BY 4.0 International license.

886 Supplementary Fig. 2

887 **Supplementary Fig. 2.** Phylogenetic tree based on 107 single copy housekeeping genes of
888 members of the Rhizobiaceae family. The *de novo* sequenced isolates CG1-CG6 are integrated
889 into a phylogenetic tree of Rhizobiaceae reference genomes from the EZBioCloud database.

bioRxiv preprint doi: https://doi.org/10.1101/2023.06.20.545721; this version posted November 21, 2023. The copyright holder for this preprint (which was not certified by peer review) is the author/funder, who has granted bioRxiv a license to display the preprint in perpetuity. It is made available under aCC-BY 4.0 International license.

Supplementary Table S1. Information on bacterial isolates of grapevine crown galls sampled from different vineyards in the Franconian region, Germany. Listed are 1. the characteristics of the isolates and 2. the relative abundance of 16S rRNA V4 amplicons in crown galls (% CG) and non-galled graft unions (% NG; Faist, et al 2017). Significant differences (p-value ≤ 0.05) between the graft unions with and without a crown gall were calculated according to one-way ANOVA followed by post hoc Tukey analysis for multiple testing.

1. Characteristics					**2. 16S rRNA V4**		
Isolate	**Tumor ID**	**Sampling date, vineyard**	**Reference strain**	**%**	**CG %**	**NG %**	**P-value**
CG1, *Allorhizobium vitis*	**A**	Jan-09-2011, Himmelstadt, Germany	*Allorhizobium vitis*, NCPPB3554(T)	99.9	11	0.3	<0.0001
CG2, *Allorhizobium vitis*	**B**	Jul-17-2013, Ravensburg, Germany	*Allorhizobium vitis*, NCPPB3554(T)	99.9	11	0.3	<0.0001
CG3, *Allorhizobium vitis*	**C**	Oct-30-2013, Himmelstadt, Germany	*Allorhizobium vitis*, NCPPB3554(T)	99.9	11	0.3	<0.0001
CG4, *Agrobacterium divergens*	**B**	July-17-2013, Ravensburg, Germany	*Rhizobium* sp., H13-3	98.8	ND	ND	ND
CG5, *Rhizobiacea sp.*	**D**	Oct-24-2012, Sommerhäuser Reifenstein, Germany	*Rhizobium* sp., H13-3	98.6	0.8	0.8	0.9
CG6, *Agrobacterium rosae*	**E**	Oct-30-2013, Himmelstadt, Germany	*Rhizobium* sp., Ch11(T)	99.7	1.5	4.5	0.2
CG7, *Pseudomonas*	**B**	July-17-2013, Ravenburg, Germany	*Pseudomonas* sp., DSM 13194(T)	99.9	15.6	0.5	<0.0001
CG8, *Rahnella*	**C**	Oct-30-2013, Himmelstadt, Germany	*Rahnella* sp., Y9602	99.9	5.5	0.4	<0.1

bioRxiv preprint doi: https://doi.org/10.1101/2023.06.20.545721; this version posted November 21, 2023. The copyright holder for this preprint (which was not certified by peer review) is the author/funder, who has granted bioRxiv a license to display the preprint in perpetuity. It is made available under aCC-BY 4.0 International license.

898 **Supplementary Table S2**. Features of the assembled draft bacterial genomes (CG1-CG8). N50
899 and N90 indexes list the length of the smallest contig that build 50% and 90%, respectively of
900 the draft genomes. cont, contig.

901

Draft genome	Total cont	Cont >1kb	20 longest cont [Mb]	Total size [Mb]	N50 [kb]	N90 [kb]	GC [%]	Largest Kmer-coverage	Overall alignment rate [%]
A. vitis CG1	427	58	5.75	6.31	457	80.5	57.4	45.7	98.53
A. vitis CG2	176	39	5.29	5.50	599	108	57.7	34.0	98.78
A. vitis CG3	212	149	2.90	6.10	89.7	24.6	57.7	14.3	86.86
A. divergens CG4	117	23	5.66	5.71	458	159	55.0	28.2	98.64
Rhizobiacea sp. CG5	223	54	5.39	6.58	262	70.2	61.5	21.5	98.74
A rosaeCG6	148	26	5.68	5.74	472	204	56.6	49.4	97.99
Pseudomonas CG7	392	182	2.48	6.87	65.5	17.6	60.7	19.6	84.98
Rahnella CG8	175	73	4.07	5.63	186	43.0	52.3	43.5	87.92

902
903

bioRxiv preprint doi: https://doi.org/10.1101/2023.06.20.545721; this version posted November 21, 2023. The copyright holder for this preprint (which was not certified by peer review) is the author/funder, who has granted bioRxiv a license to display the preprint in perpetuity. It is made available under aCC-BY 4.0 International license.

904 **Supplementary Table S3.** Bacterial growth assays in liquid medium with AB salts and
905 supplemented with either nopaline, octopine, glycerol, or sucrose+NH_4^+ as sole C and N source.
906 Optical density at 600 nm (OD_{600}) was measured after 48 h. Mean values of OD_{600} represent 5
907 replicates of two experiments. As control served the *Agrobacterium* strains C58 utilising
908 nopaline and B6 octopine. OD < 0.1, no growth; 0.1 ≤ OD < 0.2, very weak growth; 0.2 ≤ OD
909 < 0.5, weak growth; OD ≥ 0.5, growth. Red and blue colours indicate presence of isolates in
910 the same tumor.

911

Tumor			Nopaline	Octopine	Glycerol	Sucrose+NH_4^+
A	*Allorhizobium vitis*	CG1	0.37 +/- 0.12	0.58 +/- 0.16	1.42 +/- 0.17	0.85 +/- 0.00
B		CG2	0.14 +/- 0.02	0.87 +/- 0.11	1.97 +/- 0.06	3.40 +/- 0.42
C		CG3	0.26 +/- 0.07	1.14 +/- 0.42	1.98 +/- 0.03	2.10 +/- 0.07
B	*Agrobacterium divergens*	CG4	0.10 +/- 0.03	0.14 +/- 0.07	1.85 +/- 0.15	0.10 +/- 0.07
D	*Rhizobiaceae sp.*	CG5	0.15 +/- 0.03	1.01 +/- 0.25	1.92 +/- 0.04	2.68 +/- 0.04
E	*Agrobacterium rosae*	CG6	0.12 +/- 0.05	0.31 +/- 0.12	0.43 +/- 0.15	0.25 +/- 0.00
B	*Pseudomonas*	CG7	0.14 +/- 0.02	1.10 +/- 0.17	1.97 +/- 0.06	3.50 +/- 0.35
C	*Rahnella*	CG8	0.16 +/- 0.22	0.08 +/- 0.04	1.97 +/- 0.06	3.58 +/- 0.25
-	*Agrobacterium tumefaciens*	B6	0.14 +/- 0.05	0.71 +/- 0.16	1,56 +/- 0.02	2.45 +/- 0.14
-		C58	1.33 +/- 0.70	0.06 +/- 0.05	1.99 +/- 0.02	2.93 +/- 0.04
-	non-inoculated	*ni*	0.00 +/- 0.00	0.00 +/- 0.00	0.00 +/- 0.00	0.00 +/- 0.00

912

913